BASIC RESEARCH AND PERSPECTIVE TO DEVELOP TOPICAL FORMULATIONS FOR ACNE THERAPY

2015

MOHD FADLI ASMANI

BASIC RESEARCH AND PERSPECTIVE TO DEVELOP TOPICAL FORMULATIONS FOR ACNEE THERAPY

2015

MOHD FADLI ASMANI

Contents

Abbreviation

AMP	aminopyrine
BA	benzoic acid
BP	butyl paraben
Cal	calcein
CBS	carbonate buffer saline
CP	clindamycin phosphate
DFP	diisopropyl fluorophosphate
DL^{-2}	diffusion parameter
EIP	emulsion inversion point
F127	Pluronic 127
FD-4	fluorescein isothiocyanate-dextran 4 kDa
FL	fluorescein
HF	hair follicle
IP	ibuprofen
ISDN	isosorbide dinitrate
ISMN	isosorbide mononitrate
Jss	steady-state flux
KL	partition parameter
LC	lidocaine hydrochloride
P	permeability coefficient
PBS	phosphate buffered saline
PIT	phase inversion temperature
SC	stratum corneum
TEWL	transepidermal water loss
t_{lag}	lag time

Abstract

Acne vulgaris is a very common skin disease, which causes a high degree of psychosocial suffering and has a detrimental effect on the quality of life of the patients irrespective of age or gender. Treatment of acne is principally directed towards these known pathogenic factors. Clindamycin, tetracycline and erythromycin are commonly prescribed topical antibiotics for acne vulgaris with anti-inflammatory properties. However, the effectiveness of acne treatments has been limited by their relative inability to penetrate into the pilosebaceous unit, the site of acne formation.

It is very important to evaluate concentration of the therapeutic and cosmeceutical chemicals in skin because their pharmacodynamics and toxicodynamics can be expressed by a function of these concentrations. Their permeation pathway of topically applied chemical compounds, *i.e.*, stratum corneum and hair follicle (HF) is closely related to their skin concentration. Then, we aimed to investigate the contribution of skin permeation of drugs through HF as well as stratum corneum to enable their selective delivery to HF.

The contribution of HF pathway on the skin permeation of chemicals was calculated from a difference between their permeability coefficients through skin with and without HF plugging using *in vitro* skin permeation experiment. The obtained result revealed that the contribution of HF pathway could be predicted by their lipophilicities. In a hydrophilic region of chemicals ($\log K_{o/w} < 0$), a higher reduction ratio was observed by HF plugging compared with lipophilic chemicals ($\log K_{o/w} \geq 0$). In addition, the reduction ratio was decreased with an increase in the $\log K_{o/w}$. This consideration on the HF pathway

would be helpful to investigate usefulness and safety of chemicals after their topical application and exposure, because skin permeation and disposition must be changed at different sites of skin due to different sites and densities of HF. Furthermore, another study was conducted to evaluate the drug disposition in HF. HF concentration of drugs with different lipophilicities was investigated to evaluate the effect of physicochemical properties on their HF disposition, where drugs having $\log K_{o/w} < 0$ and $\log K_{o/w} \geq 0$ were assumed to be lipophilic and hydrophilic, respectively. Results showed that the lag time observed in the skin permeation before obtaining a steady-state profile for hydrophilic drugs was delayed compared with that for lipophilic drugs. Hydrophilic drugs were found to be distributed through the HF as well as into the shallow part of stratum corneum, whereas lipophilic drugs distributed both into the stratum corneum and HF from a histological observation using fluorescent makers. These results suggest that lipophilic drugs could be easily delivered both into the stratum corneum and HF, whereas hydrophilic drugs were mainly delivered through HF, but not for deep layer of the stratum corneum.

Thus, in a future study, aiming to formulate the clindamycin and tetracycline nano-emulsion by using emulsion phase inversion method to increase the effectiveness of acne treatment through the increased the penetration of the hydrophilic active compounds into the pilosebaceous unit. However, only a few studies have been focused on selective drug delivery to HF.

General introduction

Skin is the outermost and largest organ of the body; i.e., it contributes 10% of body weight and 1.7 m^2 of surface area. Skin consists of three structural layers known as, the epidermis (outer surface layer), dermis and subcutaneous tissues (deepest layer). Epidermis comprises of two different layers of epithelium, which are the viable epidermis and the stratum corneum. The viable epidermis serves as a hydrophilic layer with composition of 70% water. On the other hands, the stratum corneum composed of only 13% water and serves as a hydrophobic layer. Hydrophilic compound is not able to penetrate easily across the hydrophobic stratum corneum. Hydrophobic compounds can penetrate the stratum corneum but cannot enter the next layer of hydrophilic viable epidermis layer[1]. Dermis gives a mechanical strength to the skin as it composed of collagen fibrils embedded in mucopolysaccharide gel. In addition, the dermis contains few embedded structures including blood and lymphatic vessels, hair follicles (HF), sebaceous glands and sweat glands[2].

A topically therapeutic agent is able to penetrate through the skin via the stratum corneum[3] and skin appendages including HF[4]. The stratum corneum route can be divided into transcellular and intercellular routes. The transcellular route gives a direct penetration of drugs to cross through the stratum corneum. However, this route gives a significant resistance against drug permeation as the compound has to pass through both lipophilic and hydrophilic layers. Intercellular route is a more common pathway for drug entrance in which the compound moving between the corneocytes[5]. Recently, follicular penetration route has shown to be one of the efficient pathways for topically applied compounds[6].

Pig skin has been a well-known experimental animal skin for many years. It serves as a good representative for human model skin due to similarities in terms of physiological and anatomical points between human and pig. The decision of choosing pig ear skin in the experiments was because it represents a suitable model for human skin according to Jacobi studied in 2005[7]. Besides that, human skin has a disadvantage of becoming contracted during excision. This causes the HF to be permanently blocked the contracted elastic fibers[8]. Thus, pig ear skin can be described as a superior model to excised human skin in follicular penetration studies.

Acne vulgaris is one of the most common skin disorders in 80% of most adolescents, though it can continue to occur in adulthood especially in women due to hormonal imbalance during menstrual cycle. Comedones, inflamed papules, pustules and nodules can be observed in the lesion of acne. Acne is mostly present in the highest number of pilosebaceous glands area such as the face, chest and back[9].

The use of antimicrobial therapy or antibiotics in the treatment of acne has started since 1930s and 1940s. Although antibiotics have been a part of mainstay treatment for a long time, acne experts recommend it to act as an adjunctive therapy instead of primary in the role of acne treatment[10]. The mechanism on how topical antibiotics help to improve acne has not been clearly defined. They probably act on *Propionibacterium acne* (*P. acne*) colonization and thus produce pro-inflammatory actions on the comedogenesis. The most commonly used topical antibiotics on the acne are clindamycin, tetracycline and erythromycin[11]. However, topical gentamicin sulfate can also be used to secondary treat skin infections including pustular acne[12].

General concepts of this research are to quantitatively analyze the HF contribution pathway on the skin permeation of topically applied hydrophilic and lipophilic chemical compounds. Objective of this research is to investigate the permeation pathway of hydrophilic and lipophilic chemicals in the stratum corneum and HF for each chemical in details. Understanding the kinetic parameters in HF as well as stratum corneum will be essential for development of topical dosage forms for acne therapy

Many reports have published that skin appendages such as HF and sweat glands becomes an important permeation/penetration pathway especially of hydrophilic compounds and macromolecules. Blood and skin concentrations of topically applied or exposed chemicals can be calculated from their *in vitro* skin permeation profiles by taking into consideration of skin thickness and applying chemical concentrations. It is very important to evaluate usefulness and safety of topically applied or exposed chemicals, because their pharmacodynamics and toxicodynamics can be expressed by a function of these concentrations. Thus, permeation pathways of hydrophilic chemicals, i.e., stratum corneum and HF, should be discussed for each chemical in details. Most of the experiments were performed to identify the diffusion pathway and distribution of topically applied or exposed chemicals through and in skin by an imaging analysis using a confocal microscope

In Chapter 1, contribution to HF pathway of topically applied or exposed chemicals was determined from a difference between permeability coefficient of chemicals through skin with and without HF plugging. By concerning the topical routes of drug administration, the common skin permeation for drugs is mainly by passing through the

stratum corneum. The stratum corneum which located at the outermost layer of skin became a major barrier for drug permeation into the skin. Hence, several chemical and physical approaches have been researched to encounter the skin barrier.

In Chapter 2, drug disposition in HF is a key issue after topical application. Although dermatopharmacokinetic parameters of topically applied drugs in the stratum corneum have been evaluated using *in vitro* skin permeation experiment, *in vivo* tape-stripping technique, and so on, few studies have reported on the pharmacokinetic parameters in HFs after topical application. Understanding the dermatopharmacokinetic parameters on the HF penetration as well as stratum corneum would be essential for development of topical application forms. In the present study, HF concentration of topically applied drugs with different lipophilicities was investigated to evaluate the effect of physicochemical properties on their HF disposition.

In Appendix, development of the nano-emulsion formulations to enhance skin permeation and HF concentration after topical application was described. Nano-emulsions can be used to deliver drugs to patients via several routes. Currently the administration of drugs as in nano-emulsions via topical application has gained increasing interest. Nano-emulsions can increase the rate of absorption and eliminate variability in absorption. Hydrophilic and lipophilic drugs can also be delivered by nano-emulsions to increase their bioavailability, since the skin permeability of drugs may be affected by nano-emulsions.

Chapter 1

Contribution of hair follicular pathway of topically applied and exposed chemicals for the total skin permeation

1.1. Introduction

The body is exposed to many chemical compounds in daily life. These chemicals are mainly absorbed *via* oral, pulmonary and dermal routes, as well as through other mucosa. Among these, the dermal pathway is more easily accessed by chemicals than the other pathways because skin is the outermost tissue covering the whole body and has a large surface area[13]. The skin is also focused on as the application site of drugs and cosmetics. The pathway for the permeation of therapeutic and cosmeceutical chemicals through the skin is thus very important to evaluate their effects. In case of either skin application or skin exposure, skin permeation and the concentration of chemicals should be investigated to evaluate their effects and/or toxicities.

Skin can be histologically divided into three different layers from the surface to deeper tissues: stratum corneum, viable epidermis and dermis. The superficial layer, the stratum corneum, is composed of dead corneocytes embedded in intercellular lipid matrices consisting of ceramides, free fatty acids, cholesterol and cholesteryl esters[14]. These lipids are organized into lamella structures in the intracellular region of the stratum corneum and form the primary barrier against the elimination of endogenous compounds and the penetration of exogenous chemicals through the skin[15]. The permeation profile of chemicals through skin is theoretically expressed by Fick's 2nd law of diffusion, which

expresses the behavior of chemicals passing through the stratum corneum[9, 16]. On the other hand, many reports[17, 18, 19] have been published describing that skin appendages such as HF and sweat glands are an important permeation/penetration pathway, especially for hydrophilic compounds and macromolecules.

Many researchers have already investigated the transfollicular permeation of topically applied chemicals. Feldman *et al.*[12] and Maibach *et al.*[20] have reported that regional variation in percutaneous absorption was obtained due to different hair densities. Hueber *et al.*[21] investigated the role of HF as a skin permeation route with burn scar tissue. Grice *et al.*[22] studied the effect of drug uptake into HF on the skin permeation by a cyanoacrylate casting method. Hairy and non-hairy guinea pig skins were used for *in vivo* and *in vitro* studies to check the transfollicular absorption. Furthermore, pharmacokinetic modeling was also applied to define the relative contribution of the HF route. In addition to these skin permeation studies, the diffusion pathway and the distribution of topically applied or exposed chemicals through and in skin were identified by imaging analysis using a confocal microscope[23, 24, 1]. However, all of these studies did not involve quantitative analyses, and few studies evaluated the contribution of the HF pathway of topically applied or exposed chemicals by *in vivo* or *in vitro* skin permeation experiments[25, 11, 26].

Horita *et al.*[27] have already established a HF plugging method using cyanoacrylate-grease mixture, and then reported that the permeation of hydrophilic chemicals through HF -plugged skin was dramatically decreased, whereas lipophilic chemical permeation through HF-plugged skin was seldom changed compared with that

through non-HF-plugged skin. Otberg *et al*.[28] applied caffeine in a mixed solution of ethanol : polyethylene glycol (30 : 70 v/v) to volunteers before and after blocking all HF with a varnish solution at the site of its application. From this study, caffeine was observed in blood 20 min after application on the HF-blocked skin, but 5 min after topical application to normal skin. A possible reason for the more rapid appearance of caffeine in blood is the rapid absorption of the substance by penetrating through HF to blood capillaries. In addition, Trauer *et al*.[29] reported that the *in vivo* absorption of caffeine from whole skin was much more rapid and substantial than the *in vitro* absorption. Furthermore, a sandwich technique has been used to clarify the contribution of the HF pathway to the whole absorption of topically applied chemicals[26]. The sandwich technique revealed that the HF pathway could contribute 34% to 60% to the whole skin permeation of chemicals with different lipophilicities ($\log K_{o/w}$ range: -1.05 to 2.29) and molecular weights (*M.W.* range: 251 to 362). However, no clear relationship has been reported between physicochemical properties and the contribution of the HF pathway to whole skin permeation.

Blood and skin concentrations of topically applied or exposed chemicals can be calculated from the *in vitro* skin permeation profile by taking into consideration of the skin thickness[30] and the applied chemical concentrations. This is very important to evaluate the usefulness and safety of topically applied or exposed chemicals because their pharmacodynamics and toxicodynamics can be expressed as functions of these concentrations. Thus, the permeation pathway of hydrophilic chemicals, namely, the stratum corneum and HF, should be discussed in detail for each chemical.

The hair follicular openings occupy only about 0.1% of the whole skin area, but this can be as high as about 10% for the face around the mouth and scalp[18]. Thus, we have to take this into account in terms of the applied chemicals and the skin sites in order to evaluate the usefulness and safety of chemicals. In the present study, the contribution of the HF pathway against the whole permeation of chemicals was determined from the difference between the permeation coefficients of chemicals through skin with and without HF plugging.

1.2. Method

1.2.1. Materials

Lidocaine hydrochloride (LC), fluorescein isothiocyanate-dextran 4 kDa (FD-4), sodium calcein (Cal-Na) and ibuprofen (IP) were obtained from Sigma-Aldrich Co., Ltd. (St. Louis, MO, U.S.A.). Isosorbide dinitrate (ISDN) was kindly donated by Toko Pharmaceutical Industrial Co., Ltd. (Tokyo, Japan). Butyl paraben (BP) and isosorbide mononitrate (ISMN) were obtained from Tokyo Kasei Kogyo Co., Ltd. (Tokyo, Japan). Nile red was obtained from Kanto Chemical Co., Inc. (Tokyo, Japan). Aminopyrine (AMP) and diisopropyl fluorophosphate (DFP) were obtained from Wako Pure Chemical Ind., Ltd. (Osaka, Japan). All other reagents and solvents were of reagent grade or HPLC grade, and were used without further purification. Table 1.1 shows the physicochemical properties of the model chemicals used in the present skin permeation experiment.

Table 1.1 Physicochemical properties of drugs used in this experiment

Model drug	$M.W.$	$\log K_{o/w}$ (pH)	pK_a
FD-4	$ca.$ 4000	-0.77 (7.4) [e]	6.7 [h]
Cal-Na	644.5	-3.50 (7.4) [f]	5.5 [i]
CP	505	-2.27 (10)	6.9
FL-Na	376.3	-0.61 (7.4) [e]	6.4 [e]
ISDN	236.1	1.23 (7.4) [g]	—
LC	234.3	-0.90 (5.0)[b] 1.40 (10.0) [d]	7.9 [j]
AMP	231.3	-1.00 (3.0) [a] 0.98 (7.4) [c]	5.0 [k]
IP	206.3	1.93 (3.0) [a] 1.25 (7.4) [c]	4.9 [l]
BP	194.2	3.50 (7.4) [c]	8.3 [m]
ISMN	191.1	-0.15 (7.4) [g]	—

a) n-octanol/pH3.0 citrate buffer $\log K_{o/w}$ at 32 ℃.
b) n-octanol/pH5.0 citrate buffer $\log K_{o/w}$ at 32 ℃.
c) n-octanol/pH7.4 phosphate buffer $\log K_{o/w}$ at 32 ℃.
d) n-octanol/pH10.0 carbonate buffer $\log K_{o/w}$ at 32 ℃.
e) n-octanol/pH7.4 phosphate buffer $\log K_{o/w}$ at 32 ℃[19].
f) n-octanol/pH7.4 phosphate buffer $\log K_{o/w}$ at 32 ℃[31].
g) n-octanol/pH7.4 phosphate buffer $\log K_{o/w}$ at 32 ℃[32].
h) pK_a at 25 ℃[8].
i) pK_a at 25 ℃[33].
j) pK_a at 25 ℃[6].
k) pK_a at 25 ℃[34].
l) pK_a at 25 ℃[10].
m) pK_a at 25 ℃[4].

1.2.2. Determination of n-octanol /buffer partition coefficient

n-Octanol was saturated with pH3.0 citrate buffer, pH5.0 citrate buffer, pH7.4 phosphate buffer or pH10.0 carbonate buffer for at least 24 h before the partition experiment at 37°C. Drug was dissolved in *n*-octanol-saturated buffered solution. The obtained solution was mixed with an equal volume of buffer solution-saturated *n*-octanol at 37°C for 24 h. Drug concentration in the aqueous phase was then analyzed by HPLC. Apparent *n*-octanol/buffer solution partition coefficients ($K_{o/w}$) were determined.

1.2.3. Animals

Frozen pig ear skins were purchased from the National Federation of Agricultural Cooperative Associations (Tokyo, Japan). These skins were stored at -30°C until the skin permeation experiments. All animal studies were carried out with the recommendations of the Institutional Board for Animal Studies, Josai University (Sakado, Saitama, Japan).

1.2.4. Preparation of skin membrane

Purchased skin was frozen at -80°C prior to use. The skin was thawed at room temperature and excised from the outer surface of pig ear after being cleaned with pH7.4 phosphate buffered saline (PBS). The excised skin was mounted on a Franz-type diffusion cell to conduct the skin permeation study. In the case of skin permeation study with HF-plugged skin, the plugging procedure was carried out after skin excision. The integrity of the excised skin was measured using a skin impedance meter 1 h after hydration with 1 mL

of PBS and all of the skin samples used in the present study showed resistance of above 20 kohm/cm^2.

1.2.5. Hair follicle-plugging process

The HF-plugging procedure was as previously reported in detail (Horita *et al*., 2014). This procedure can be briefly summarized as follows. HF in the designated area (effective skin permeation area: 1.77 cm^2) were plugged with silicone grease-cyanoacrylate adhesive mixture paste to block chemical penetration through the HF. The mixture paste consisted of equal parts of silicone grease (Super Lube$^®$ Silicone Dielectric Grease; Synco Chemical Corp., Bohemia, NY, U.S.A.) and α-cyanoacrylate adhesives (Aron Alpha Jelly; Konishi Co., Ltd., Osaka, Japan) with small amounts of Nile red. Nile red was used to visualize the area to which the mixture paste had been applied. Thus, the HF were plugged with the mixture paste to prevent chemical penetration through the follicular pathway. A mean of 56.1 ± 2.5 HF (n=15) were found in the effective pig ear skin permeation area (1.77 cm^2) in the preliminary experiment, and half of them were plugged with the mixture paste in the present experiment. According to Horita *et al*.[27], an almost linear decrease in the skin permeation ratio was observed with an increase in the number of HF plugged with the mixture paste. The mixture paste-treated area was measured using imaging software (cellSens, Olympus Corp., Tokyo, Japan), equipped with a stereoscopic microscope (SZ61, Olympus Corp., Tokyo, Japan). The effective skin permeation area was about 1.62 cm^2 after treatment with the mixture paste. Figure 1.1 shows the skin surface with or without the HF plugging.
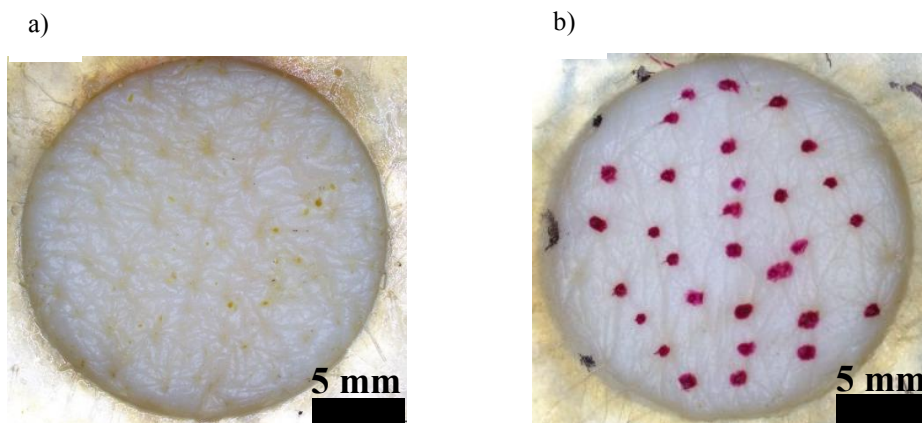
Fig.1.1. Pictures of the pig ear skin surface with (a) or without (b) HF plugging.

1.2.6. Preparation of applied solution

First, 5.0 mM FD-4, 1.0 mM FL-Na, 5.0 mM ISDN, 10 mM non-ionized AMP, 5.0 mM ionized IP, 0.6 mM BP and 500 mM ISMN were prepared with 1/30 mM PBS (pH7.4). Then, 1.0 mM Cal-Na was prepared with pH7.4 PBS containing 1.0 mM EDTA-2Na. In addition, 10 mM non-ionized LC was prepared with 100 mM carbonate-bicarbonate buffer solution (pH10.0) and 100 mM ionized LC was prepared with 100 mM citrate buffer solution (pH5.0). Furthermore, 100 mM ionized AMP and 0.5 mM non-ionized IP were prepared with pH3.0 citrate buffer. The pH levels for the fluorescent compounds such as FD-4, Cal-Na and FL-Na and weak electrolytes except for BP were adjusted to ensure that about 99% were in non-ionized or ionized form.

1.2.7. In vitro skin permeation experiments

Excised pig ear skin membrane was mounted on vertical-type diffusion cells

(effective diffusion area: 1.77 cm^2). The stratum corneum was hydrated for 1 h with pH-adjusted solution or PBS containing 2.7 μmol/mL DFP. The latter was used to prevent the metabolism of ester compounds during the skin permeation experiment. It has already been confirmed that the hydration procedures with DFP did not affect the skin permeation of the esters and their metabolites [35-37].

After the pre-hydration process, solution applied to the skin was completely removed from the diffusion cell and 1.0 mL of test chemical solution and 6 mL of pH-adjusted solution were applied to the donor and receiver cells, respectively. The total of 0.54 μmol/mL DFP was added on the dermis side when ester compounds were applied on the stratum corneum. The permeation experiments were performed at 32°C, while the receiver solution was continuously stirred with a star-head-type magnetic stirrer. At predetermined times, an aliquot (0.5 mL) was withdrawn from the receiver solution and an identical volume of fresh solution was added to keep the volume constant. Each experiment was performed in 3 to 4 replicates.

1.2.8. Determination of FD-4 and FL using a spectrofluorophotometer

The concentrations of FL, Cal and FD-4 in the samples were analyzed using a spectrofluorophotometer (RF 5300PC; Shimadzu) at excitation wavelengths of 480 nm, 488 nm and 490 nm, and at fluorescent emission wavelengths of 535 nm, 515 nm and 520 nm, respectively.

1.2.9. Determination of drugs using an HPLC system

Concentrations of drugs (LC, ISDN, AMP, IP, BP and ISMN) in the samples were determined using an HPLC system (Prominence; Shimadzu, Kyoto, Japan) equipped with a UV detector (SPD-M20A; Shimadzu). The drug samples (0.2 mL) were added to the same volume of acetonitrile for ISMN or acetonitrile containing internal standard (methyl paraben for LC, butyl paraben for ISDN, AMP and IP, and propyl paraben for BP), and mixed with a vortex mixer. After centrifugation at $3600 \times g$ and 4°C for 5 min, 20 µL of the supernatant was injected into the HPLC system. Chromatographic separation was performed using an Inertsil-ODS-3 (5 µm, 150×4.6 mm i.d.; GL Science, Kyoto, Japan) at 40°C. The mobile phase was 0.1% phosphoric acid containing 5 mM sodium 1-heptanesulfate/acetonitrile (70/30, v/v) for LC, water/acetonitrile (55/45, v/v) for ISDN, 0.1% phosphoric acid containing 5 mM sodium dodecyl sulfate/acetonitrile (30/70, v/v) for AMP, 0.1% phosphoric acid/acetonitrile (55/45, v/v) for ISMN and water/acetonitrile (90/10, v/v) for ISMN. The flow rate was adjusted to 1.0 mL/min and detection was performed at UV 220 nm (ISMN and ISDN), 230 nm (LC), 245 nm (AMP), 260 nm (BP) or 263 nm (IP).

1.2.10. Analysis of permeation parameters

Skin permeation parameters were calculated using time courses of the cumulative amounts of chemicals that permeated through a unit area of skin with or without HF plugging. The steady-state flux (*Jss*) (a steady state was reached 6–10 h after starting the experiment) was estimated from the slope of the linear portion of the profile of the cumulative amount of chemical that permeated through a unit area of skin versus time,

and the lag time (t_{lag}) was calculated from the intercept on the time axis by extrapolation from the steady-state skin permeation profile. From Jss and the initial donor concentration (C_v), the permeability coefficient (P) was calculated using eq. 1. The partition parameter (KL) and the diffusion parameter (DL^{-2}) were then obtained from eqs. 2 and 3 [38]:

$$P = \frac{J}{C_v} \qquad (1)$$

$$t_{lag} = \frac{L^2}{6D} \qquad (2)$$

$$P = KL \cdot DL^{-2} \qquad (3)$$

where L, D and K are the thickness of the barrier membrane, the diffusion coefficient of chemicals in the membrane and the partition coefficient of chemicals into the membrane, respectively. DL^{-2} was obtained from eq. 2 and KL was calculated from P and DL^{-2} values according to eq. 2.

In addition, the reduction ratio of P of topically applied chemicals due to HF plugging was calculated using eq. 4.

$$Reduction\ ratio = \left(\frac{P_{through\ nonplugged\ skin} - P_{through\ plugged\ skin}}{P_{through\ nonplugged\ skin}} \right) \times 100 \qquad (4)$$

Then, the contribution of the HF pathway to the whole skin permeation of chemicals was obtained by doubling the reduction ratio shown in the figure, since plugging of 30 of the total of 60 HF in the effective skin area had been carried out.

1.2.11. *Statistical analysis*

Statistical analysis was performed using unpaired Student's *t*-test and ANOVA.

p value of less than 0.05 was considered significant.

1.3. Results

1.3.1 Effect of pH on the skin permeation of ISDN

Figure 1.2 shows the time course of the cumulative amount of ISDN that permeated through pig ear skin from its solution with different pH levels (pH3.0, 7.4 and 10.0) in order to investigate the effect of pH on the skin permeation of the neutral drug. As expected, almost the same ISDN permeation profiles were obtained independently of the pH under these experimental conditions. In addition, skin permeation parameters of t_{lag}, DL^{-2} and KL obtained from the skin permeation profiles of ISDN for pH3.0 and pH10 solutions were very similar to those for the pH7.4 solution (Table 1.2).

Table 1.2 Skin permeation parameters of ISDN from solutions with different pHs

	pH3.0			pH7.4			pH10.0		
Q_6 (μmol/cm^2)$^{\#}$	1.30×10^{-1}	$\pm$	1.64×10^{-2}	1.19×10^{-1}	$\pm$	2.18×10^{-2}	1.22×10^{-1}	$\pm$	1.11×10^{-2}
P (cm/s)	2.46×10^{-6}	$\pm$	4.67×10^{-7}	2.01×10^{-6}	$\pm$	2.93×10^{-7}	1.86×10^{-6}	$\pm$	2.34×10^{-7}
t_{lag} (h)	1.91	$\pm$	0.23	2.22	$\pm$	0.16	2.02	$\pm$	0.21
DL^{-2} (cm^{-1})	1.02×10^{-1}	$\pm$	1.25×10^{-2}	7.56×10^{-2}	$\pm$	5.36×10^{-3}	8.42×10^{-2}	$\pm$	8.27×10^{-3}
KL (cm)	2.35×10^{-5}	$\pm$	2.74×10^{-6}	2.62×10^{-5}	$\pm$	2.24×10^{-6}	2.30×10^{-5}	$\pm$	5.03×10^{-6}

#Q_6: Cumulative amount of ISDN that permeated through the skin over 6 h.
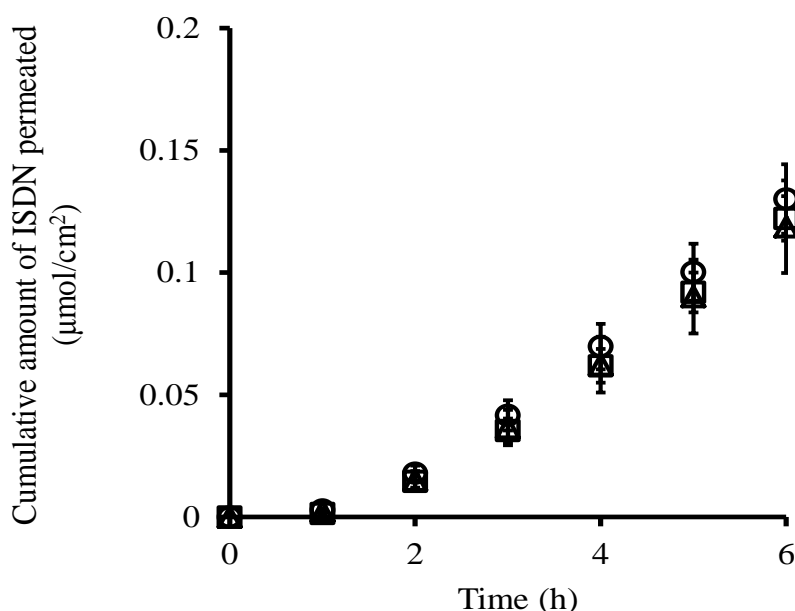
Fig.1. 2. Time course of the cumulative amount of ISDN that permeated through pig ear skin from its solution. pH3.0 ($\bigcirc$), pH7.4 ($\triangle$) and pH10.0 ($\square$). Each point represents the mean $\pm$ S.D. (n = 3-4).

1.3.2 Effect of hair follicle plugging on the skin permeation of drugs

Figures 1.3a and b show the effect of HF plugging on the skin permeation of ionized and non-ionized AMP, respectively. The cumulative amount of ionized AMP (at pH3.0) that permeated through the plugged skin was about half that through the non-

plugged skin (Fig. 1.3a). On the other hand, the cumulative amount of non-ionized AMP (at pH7.4) that permeated through the plugged skin was about 0.7-fold that through the non-plugged skin (Fig. 1.3b). The sizes of these decreases in the cumulative amount of AMP that permeated were greatly affected by the ratio of ionized to non-ionized forms. Table 3 shows permeation parameters calculated from the skin permeation profiles shown in Fig. 1.3. These parameters can be utilized to evaluate the changes in distribution and/or diffusion of topically applied or exposed chemicals to and across the skin [19, 39]. The KL values obtained through the HF plugging were decreased at both pH3.0 and pH7.4 compared with those of non-plugged skin, although the DL^{-2} values were almost the same. These decreased KL values at both pH3.0 and pH7.4 corresponded to the sizes of the decreases in the cumulative amount of AMP that permeated through the plugged skin compared with the non-plugged skin.

Table 1.3 Skin permeation parameters and reduction ratio of AMP with or without HF-plugged skin

		Non-HF plugging		HF plugging		Ratio[#]
pH3.0	Q_{10} (μmol/cm^2)	2.40×10^{-2}	$\pm$ 7.55×10^{-3}	1.17×10^{-2}	$\pm$ 4.41×10^{-3}	0.49
	P (cm/s)	8.70×10^{-9}	$\pm$ 2.38×10^{-9}	4.73×10^{-9}	$\pm$ 2.02×10^{-9}	0.54
	t_{lag} (h)	2.53	$\pm$ 0.5	2.56	$\pm$ 0.4	1.01
	DL^{-2} (h^{-1})	1.17×10^{-4}	$\pm$ 2.32×10^{-5}	1.19×10^{-4}	$\pm$ 1.86×10^{-5}	1.02
	KL (cm)	7.58×10^{-5}	$\pm$ 2.00×10^{-5}	3.99×10^{-5}	$\pm$ 1.70×10^{-6}	0.52
pH7.4	Q_{10} (μmol/cm^2)	3.78×10^{-2}	$\pm$ 1.41×10^{-3}	2.73×10^{-2}	$\pm$ 2.11×10^{-3}	0.72
	P (cm/s)	1.61×10^{-7}	$\pm$ 8.10×10^{-9}	1.43×10^{-7}	$\pm$ 1.61×10^{-8}	0.89
	t_{lag} (h)	3.85	$\pm$ 0.14	4.18	$\pm$ 0.24	1.09

DL^{-2} (h^{-1})	1.78×10^{-4}	$\pm$	6.34×10^{-6}	1.94×10^{-4} $\pm$ 1.11×10^{-5}	1.09
KL (cm)	9.06×10^{-4}	$\pm$	5.05×10^{-5}	7.51×10^{-4} $\pm$ 1.05×10^{-4}	0.83

Ratio#: HF plugging/non-HF plugging
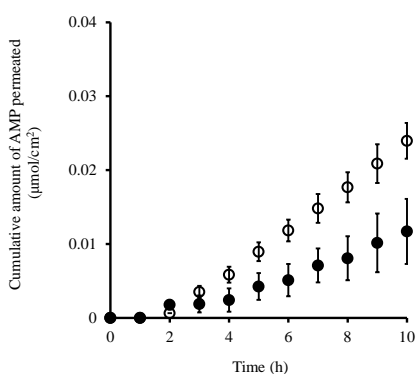
(a)   (b)
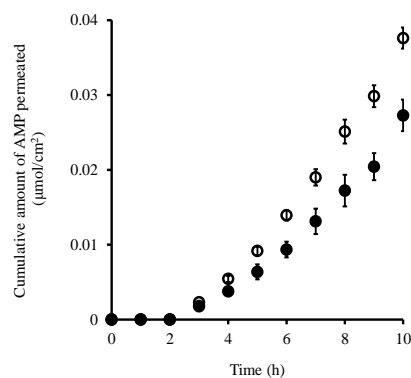
Fig.1.3. Time course of the cumulative amount of AMP that permeated through pig ear skin at pH3.0 (a) and pH7.4 (b). Non-HF-plugged skin (○), HF-plugged skin (●). Each point represents the mean ± S.D. (n = 4).

Next, a skin permeation experiment for several chemicals was carried out with or without HF plugging to determine their *P* values as listed in Table 1.4. This table also shows the reduction ratio of *P* values calculated using eq.4. Reductions of the *P* value of around 50% were observed for FD-4, Cal-Na, FL-Na, ionized LC, ionized AMP and ISMN,

whereas no or only slight reductions (less than 20%) in P value were observed for non-ionized BP, non-ionized IP and non-ionized LC. Furthermore, reduction ratios of P values of 20% to 40% were shown for non-ionized AMP, ionized IP and ISDN.

Table 1.4 Reduction in permeability coefficient of chemicals through the HF-plugged skin. Values are the mean ± S.E. (n = 3-4).

	pH of applied solution	P values through HF-non-plugged skin (×10^{-8} cm/s)	P values through HF-plugged skin(×10^{-8} cm/s)	Reduction ratio (%)
FD-4	7.4	0.064 ± 0.032	0.026 ± 0.012	59
Cal-Na	7.4	2.8 ± 1.2	1.4 ± 1.7	50
CP	10.0	3.2 ± 0.68	1.2 ± 0.12	61
FL-Na	7.4	1.4 ± 0.57	0.62 ± 0.089	56
ISDN	7.4	371 ± 122	242 ± 65	35
Ionized LC	5.0	2.3 ± 0.61	1.1 ± 0.31	52
Non-ionized LC	10.0	255 ± 109	210 ± 49	18
Ionized AMP	3.0	0.88 ± 0.48	0.46 ± 0.42	48
Non-ionized AMP	7.4	17 ± 0.74	13 ± 0.50	24
Non-ionized IP	3.0	1520 ± 270	1300 ± 81	14
Ionized IP	7.4	87 ± 16	59 ± 5.4	32
Non-ionized BP	7.4	132 ± 50	132 ± 143	0
ISMN	7.4	8.9 ± 1.2	4.9 ± 3.6	45

1.3.3 Factors of skin permeation reduction by hair follicle plugging

Figure 1.4 shows the relationship between the molecular weight of topically applied chemicals and the reduction ratio of P values by HF plugging. A reduction ratio of P values of around 50% was observed for chemicals with a molecular weight greater than 400 Da. The reduction ratio of P values seems to increase with an increase in the

molecular weight in the range from 200 to 400 Da, but the relationship between the reduction ratio of the *P* value of chemicals and their molecular weights was inconsistent, especially from 200 to 350 Da.
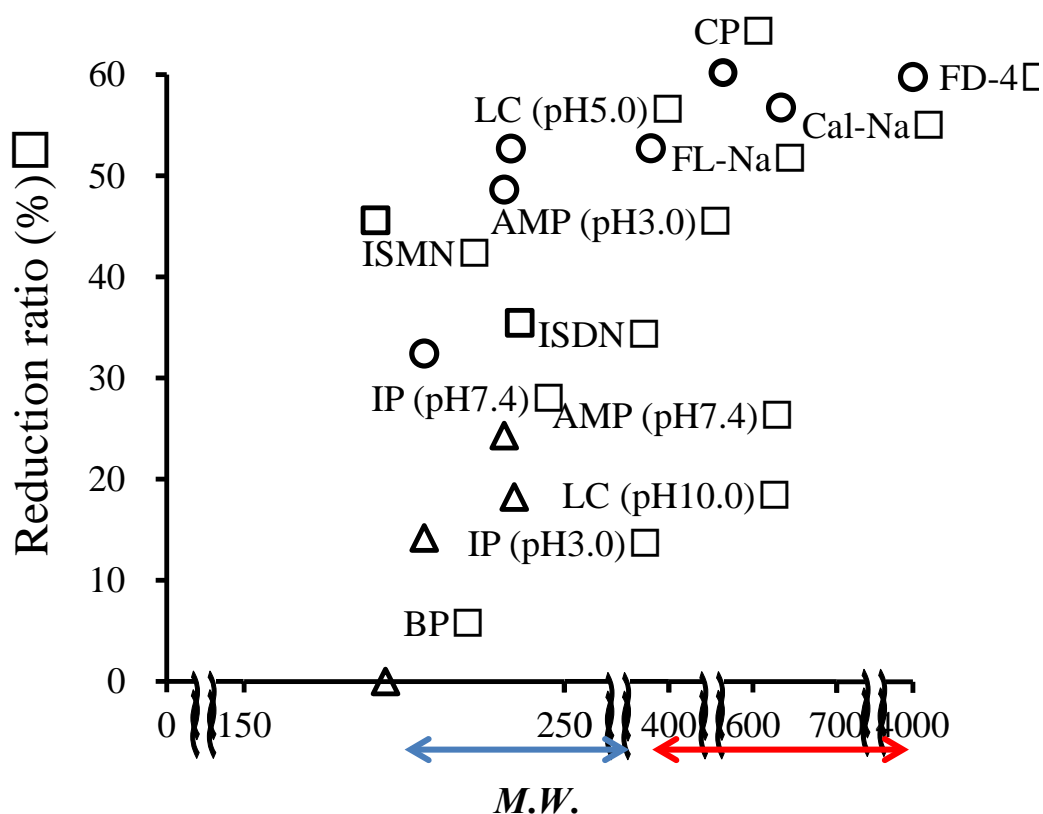

Fig. 1. 4. Relationship between the reduction ratio of skin permeation by HF plugging and the molecular weight of the chemicals. ○: ionized form (acidic or basic chemicals), △: non-ionized form (acidic or basic chemicals), □: neutral chemicals.

Next, the effect of the lipophilicity of chemicals, $\log K_{o/w}$, on the reduction ratio of the P value was investigated. Figure 1.5 shows the relationship between the reduction ratio of the P value of chemicals and their $\log K_{o/w}$ values. For hydrophilic chemicals ($\log K_{o/w} < 0$), a higher reduction ratio was observed than for lipophilic ones ($\log K_{o/w} \geq 0$). In addition, the reduction ratio decreased with an increase in $\log K_{o/w}$. Furthermore, about a 10% reduction of chemical permeation was evenly observed for every 1.0 $\log K_{o/w}$ increase of chemicals (i.e., every 10-fold increase in $K_{o/w}$ value) within the range of $\log K_{o/w}$ values from 0 to 4.
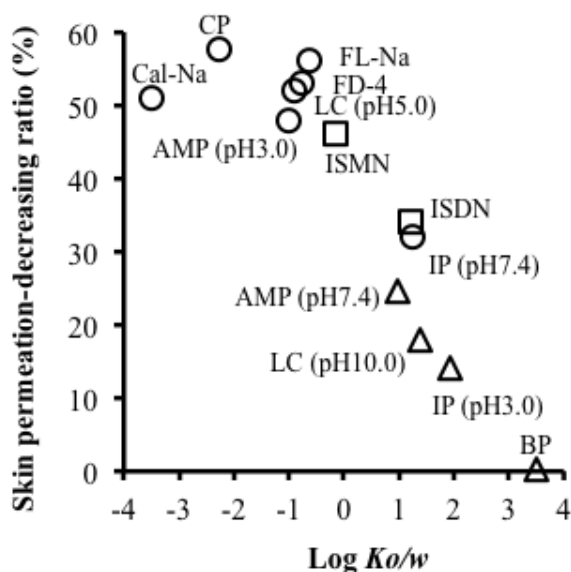

Fig .1.5. Relationship between the reduction ratio of skin permeation by HF plugging and the partition coefficient of the chemicals. ○: ionized form (acidic or basic chemicals), △: non-ionized form (acidic or basic chemicals), □: neutral chemicals.

1.4. Discussion

Generally, blood and skin concentration profiles of topically applied or exposed chemicals or drugs can be calculated from the *in vitro* skin permeation profile[40), 41), 42)]. Presently, the calculation method is especially applicable for chemicals for which the main permeation route is the stratum corneum. If the contribution of HF to the total skin permeation of chemicals can be obtained, blood and skin concentrations of drug would be more precisely predicted. Since excised skin used in an *in vitro* study might show a histological reduction in the follicular penetration pathway via contraction of the elastic fibers surrounding HF, Patzelt *et al.*[43)] speculated that an *in vitro* skin permeation experiment may not be suitable for determining the contribution of the HF pathway to the total skin permeation of chemicals. On the other hand, Raber *et al.*[44)] reported an excellent *in vivo*/*in vitro* correlation in terms of the nanoparticles level recovered from HF after their topical application. *In vitro* skin permeation experiments have already been broadly used to evaluate and develop transdermal drug delivery systems (TDDS). Furthermore, there are ethical issues associated with *in vivo* experiments, especially regarding the development of cosmeceutical products. Therefore, in the present study, an *in vitro* experiment was carried out to determine the contribution of the HF pathway.

According to Horita *et al.*[27)], a good linear regression was obtained between the decrease in the skin permeation of a high-molecular-weight chemical, FD-4, and the number of HF plugged. About 58 visible HF were confirmed in an effective skin permeation area of 1.77 cm^2. The point at which the regression line crossed the x-axis showed that plugging of 28 and 58 HF led to decreases in the skin permeation of FD-4 of

50 and 100 percent, respectively. Furthermore, no permeation of FD-4 or FL-Na was observed through three-dimensional cultured human skin models[19]. This is because the cultured human skin models have no HF. Thus, the present results strongly suggest that the HF pathway is the primary pathway of FD-4 and FL-Na through the skin. Thirty HF in the effective skin permeation area were plugged in this study to calculate the contribution of the HF pathway to the whole skin permeation of topically applied or exposed chemicals.

Among the present results, only KL parameters were decreased by HF plugging, while the values of DL^{-2} were almost constant after the application of AMP solution at different pH levels, suggesting that the plugging method could enable evaluation of the contribution of the HF pathway to the total skin permeation of chemicals. The fraction of HF in a diffusion area should be related to the partition parameter of chemicals when HF are its main permeation route[19]. Therefore, the present plugging method should be useful for calculating the contribution of HF to the permeation of topically applied or exposed chemicals.

Figure 1.6 shows the relationship between the contribution of the HF pathway and the partition coefficient of chemicals. The contribution of the HF pathway was also compared with other published data to verify our results. Frum *et al.*[26] reported the influence of $\log K_{o/w}$ on HF penetration by an *in vitro* sandwich method. The percentage contribution by follicles decreased with an increase in the lipophilicity of topically applied or exposed compounds, and the levels of contribution (4%, 2%, 46%, 60%, 58%, 46% and 34% for estradiol [$\log K_{o/w}$: 2.29], corticosterone [$\log K_{o/w}$: 1.94], hydrocortisone [$\log K_{o/w}$: 1.60] and aldosterone [$\log K_{o/w}$: 1.08], respectively) were almost the same as our calculated

values. On the other hand, a downward parabolic relationship was observed for the hydrophilic compounds (58, 48 and 34% for cimetidine [$\log K_{o/w}$: 0.40], deoxyadenosine [$\log K_{o/w}$: 0.40] and adenosine [$\log K_{o/w}$: -1.05], respectively).

These data are very different from my calculated values. Frum et al.[26] calculated the HF contribution from a 28 or 48 h-skin permeation experiment. Excess hydration of the stratum corneum may change the skin characteristics by causing swelling and the development of water pools in the intercellular lamellar region[45]. This might be a reason for the low contribution of the HF pathway for hydrophilic drugs compared with the present results. Furthermore, the formulation of topically applied drugs would also affect the contribution of the HF pathway due to variation in the partitioning of chemicals in skin. Liu et al. [25] reported that caffeine ($\log K_{o/w}$: -0.01) was absorbed through HF within 30 min after topical application in a binary solvent of 30% ethanol and 70% propylene glycol, and that 10.5% to 33.8% of the total amount was absorbed through the HF.

This binary solvent could increase the skin permeation of chemicals by causing variation in the fluidity of the stratum corneum lipids. However, a much higher contribution of HF (over 90%) was obtained from aqueous solution in the present study. Thus, differences in the formulation should be an important issue to determine the contribution of HF to the permeation of topically applied or exposed chemicals.
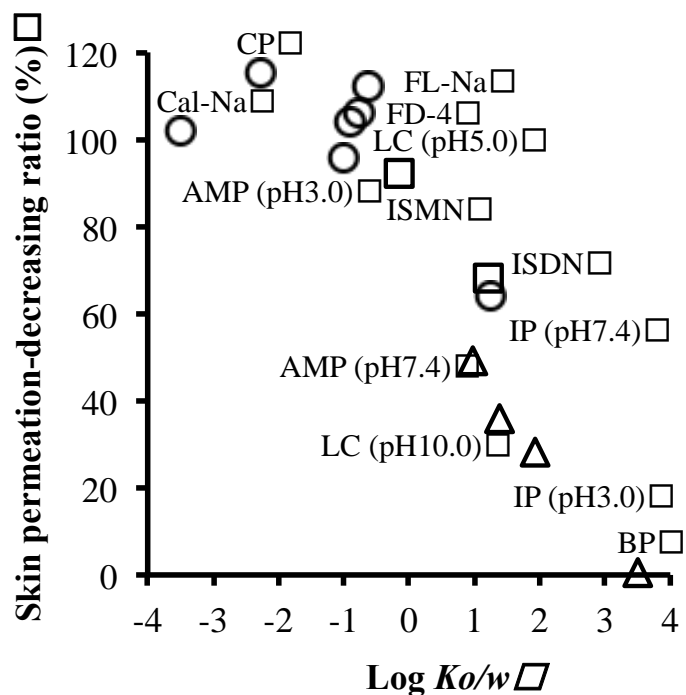
Fig.1.6. Relationship between the contribution of the HF pathway and the partition coefficient of the chemicals. ○: ionized form (acidic or basic) chemicals, △: non-ionized form (acidic or basic) chemicals, □: neutral chemicals.

This report reveals that the contribution of the HF pathway to the total skin permeation of topically applied or exposed chemicals could be calculated by using their lipophilicity. Molecular weight, lipophilicity, number of hydrogen donors or acceptors, electron affinity, charge densities, and atomic and molecular orbits (LUMO/HOMO) are also very important for the skin permeation of chemical compounds[3, 5, 7, 44, 45]. More precise estimation might thus be possible by considering these parameters.

1.5. Chapter conclusion

This chaptershows that the contribution of the HF pathway to the total skin permeation of chemicals can be determined by using their lipophilicity. Consideration of the HF pathway would be helpful to investigate the usefulness and safety of chemicals after their topical application because skin permeation and disposition would vary among different sites of skin due to the differences in the character and/or density of HF.

Chapter 2

Evaluation of drug disposition in hair follicles after topical application

2.1. Introduction

Drug concentration at target sites is very important to expect the pharmacological effect. Therefore, optimization of drug formula and formulation design should be conducted to effectively deliver an adequate amount of drug to the target site. In the 1st chapter, HF route showed higher contribution for hydrophilic drugs against the total skin permeation compared for lipophilic drugs. Hydrophilic acne treatment agents such as clindamycin, gentamycin sulfate and tetracycline hydrochloride, therefore, could be delivered to HF. The total skin permeation of hydrophilic drugs is normally lower than that of lipophilic ones, and the cumulative amount of drug permeated through skin was increased with an increase of lipophilicity. In addition, drug concentration has a very close relation to its skin permeation. Sugibayashi *et al.*[32], reported that skin concentration of topically applied drugs could be calculated with permeation parameters such as partition coefficient and permeability coefficient obtained from drug permeation profiles thorough full-thickness and stripped skins.

To develop the formulation and structure for topically applied drugs such as local anesthesia, painless and atopic dermatitis treatments, several method like suction blister[46-48], punch and shave biopsies[47,48], tape-stripping[49-51], heat-separation[52,53], autoradiography[54] methods have been used to determine drug concentration at target site in the skin. On the other hand, few studies have published on the drug concentration profiles

in the HF after topical application, although pharmacokinetics at the target site is important for drug discovery and development,
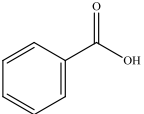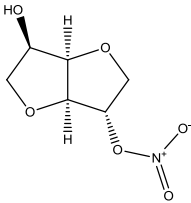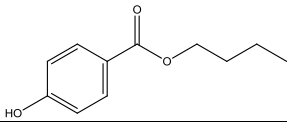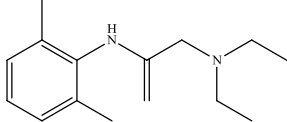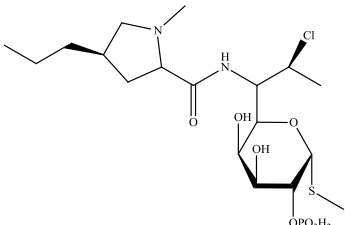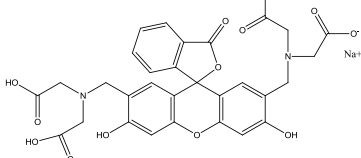
Thus, in the 2nd chapter, HF concentration after topical application of drugs with different physicochemical properties was considered to estimate the effect of lipophilicity of topically applied drugs on its steady-state concentration in HF and related pharmacokinetics.

2.2. Methods

2.2.1. Materials and methods

Isosorbide-5-mononitrate (ISMN), butyl paraben (BP), clindamycin phosphate (CP) and sodium calcein (Cal-Na) were purchased from Tokyo Chemical Industry Co., Ltd. (Tokyo, Japan). Benzoic acid (BA) and diisopropyl fluorophosphates (DFP) were purchased from Wako Pure Chemical Industries, Ltd (Osaka, Japan). Lidocaine hydrochloride monohydrate (LC) was purchased from Sigma-Aldrich (St. Louis, MO). The other solvents and reagents were of HPLC grade and regent grade-purity. All reagents were commercially available and used without further purification. Table 2.1 shows chemical structures, molecular weights ($M.W.$), n-octanol/water coefficients ($\log K_{o/w}$) and acid dissociation constant (pKa). In the present study, chemicals were classified into lipophilic and hydrophilic chemicals according to their $\log K_{o/w}$ values; chemicals with $\log K_{o/w}$ values greater than 0 are regarded as lipophilic drugs and those with $\log K_{o/w}$ values less than 0 are considered hydrophilic drugs.

Table 2.1. Chemical structures and physicochemical properties of model permeants.

Drug	Chemical structure	M.W.	Log$K_{o/w}$	pK_a
Benzoic acid (BA)		122.1	1.90 (pH 3.0) [a] -0.41 (pH 7.4) [c]	4.2 [f]
Isosorbide mononitrate (ISMN)		191.1	-0.20 (pH 7.4) [c]	-
Butyl paraben (BP)		194.2	3.50 (pH 7.4) [c]	8.3 [g]
Lidocaine (LC)		234.3	-0.90 (pH 5.0) [b] 1.40 (pH 10.0) [d]	7.9 [h]
Clindamycin phosphate (CP)		505.0	-2.27 (pH 10.0) [d]	6.9 [i]
Sodium calcein (Cal-Na)		644.5	-3.51 (pH 7.4) [e]	5.5 [j]

a) *n*-octanol/pH 3.0 citrate buffer log$K_{o/w}$ at 32ºC.

b) *n*-octanol/pH 5.0 citrate buffer log$K_{o/w}$ at 32ºC.

c) *n*-octanol/pH 7.4 phosphate buffer log$K_{o/w}$ at 32ºC.

d) *n*-octanol/pH 10.0 carbonate buffer log$K_{o/w}$ at 32ºC.

e) from Ref. [55].

f) from Ref. [56].

g) from Ref. [57].

h) from Ref. [58].

i) from Ref. [59].

j) from Ref. [60].

2.2.2. Determination of n-octanol / buffer partition coefficient

n-Octanol was saturated with various pH buffer solutions as follow: pH3.0 citrate buffer, pH 5.0 citrate buffer, pH 7.4 phosphate buffered saline (PBS) or pH 10.0 carbonate-bicarbonate buffer for at least 24 h before starting the experiment at 37 °C. Each drug was dissolved in *n*-octanol-saturated buffered solution. The obtained solution was mixed with an equal volume of buffer solution-saturated *n*-octanol at 37 °C for 24 h. Drug concentration in the aqueous phase was then analyzed with HPLC. Apparent *n*-octanol / buffer solution partition coefficients ($K_{o/w}$) were then determined.

2.2.3. Animals

Frozen pig ear skin samples were purchased from the National Federation of Agricultural Cooperative Associations (Tokyo, Japan). These skin samples were stored at -30°C until the skin permeation experiments. All animal studies were carried out with the recommendations of the Institutional Board for Animal Studies, Josai University (Sakado, Saitama, Japan).

2.2.4. Preparation of skin membrane

Purchased skin was maintained as frozen at -30°C prior to use. The skin was thawed at room temperature and excised from the outer surface of pig ear skin after being cleaned with the same buffered solution to be applied in skin permeation study. The excised skin was mounted on a Franz-type diffusion cell to conduct skin permeation study. The same buffered solutions used in the skin permeation study were applied for 1 h to the

hydrate stratum corneum. To avoid hydrolysis by esterase in skin, 2.7 mM diisopropyl fluorophosphates (DFP), a serine protease inhibitor, was included in the buffer solution for 1 h. No skin permeation changes were appeared for 1 h treatment with DFP [61-63].

2.2.5. *Preparation of applied solution*

30 mM ionized BA, 50 mM ISMN, 0.5 mM BP and 1 mM Cal-Na were prepared with 1/30 mM PBS (pH 7.4). In addition, 10 mM non-ionized LC and 100 mM CP were prepared with 100 mM carbonate-bicarbonate buffer (pH10.0) and 100 mM ionized LC and non-ionized BA were prepared with 100 mM citrate buffer (pH5.0).

2.2.6. *In vitro skin permeation study*

After the pre-hydration process, applied solution to the skin was completely removed from the diffusion cell and 1.0 mL of test chemical solution and 6 mL of pH-adjusted solution were applied to the donor and receiver cells, respectively. A total of 0.54 μmol/mL DFP was added on the dermis side when ester compounds were applied on the stratum corneum. The permeation experiments were performed at 32°C, while the receiver solution was continuously stirred with a star-head-type magnetic stirrer. At predetermined times, an aliquot (0.5 mL) was withdrawn from the receiver solution and an identical volume of fresh solution was added to keep the volume constant. Each experiment was performed in 3 to 4 replicates.

2.2.7. *Estimationdrug concentration in hair follicles*

After *in vitro* skin permeation study, the skin was removed carefully from the diffusion cell after the applied solution containing drug was recovered. Then, the stratum corneum and dermis sides were washed 3 times, respectively, with 1.0 mL of the same pH-adjusted solution used to skin permeation study. Thirty hairs were removed from the effective skin permeation area with forceps under a stereoscopic microscope observation. The removed hairs with follicle tissue were measured by weight and vortexed for 20 min in 400 µL of pH-adjusted buffer solution. The solution was centrifuged (CT15RE®, Hitachi Koki Co., Ltd., Tokyo, Japan) at 15,000 rpm for 4 min at 4ºC, drug concentration in the obtained supernatant was measured with HPLC or spectrofluorophotometer. Apparent drug concentration inHF was calculated from the obtained drug amount with the hair removed from the drug-treated skin. This apparent drug concentration (drug amount/hair weight%) was assumed to "that in HF" (see discussion in detail).

2.2.8. *Determination of Cal using a spectrofluorophotometer*

The concentrations of Cal in the samples were analyzed using a spectrofluorophotometer (RF 5300PC; Shimadzu) at an excitation wavelength of 488 nm and at a fluorescent emission wavelength of 515 nm.

2.2.9. *Determination of drugs using an HPLC system*

Concentrations of drugs (LC, ISDN, BA, CP, BP and ISMN) in the samples were determined using an HPLC system (Prominence; Shimadzu, Kyoto, Japan) equipped with a

UV detector (SPD-M20A; Shimadzu). The drug samples (0.2 mL) were added to the same volume of acetonitrile for ISMN and CP or acetonitrile containing internal standard (methyl paraben for LC, butyl paraben for ISDN, BA for ethyl paraben, and propyl paraben for BP), and mixed with a vortex mixer. After centrifugation at 3600×g and 4°C for 5 min, 20 μL of the supernatant was injected into the HPLC system. Chromatographic separation was performed using an Inertsil-ODS-3 (5 μm, 150×4.6 mm $i.d.$; GL Science, Kyoto, Japan) at 40°C. The mobile phase was 0.1% phosphoric acid containing 5 mM sodium 1-heptanesulfate/acetonitrile (70/30, v/v) for LC, water/acetonitrile (55/45, v/v) for ISDN, 0.1% phosphoric acid/acetonitrile (55/45, v/v) for BA and BP and water/acetonitrile (90/10, v/v) for ISMN, 100 mM KH_2PO_4 (pH 2.5)/acetonitrile (80/20, v/v) for CP. The flow rate was adjusted to 1.0 mL/min and detection was performed at UV 220 nm (ISMN and ISDN), 230 nm (LC), 210 nm (CP), 260 nm (BP) or 254 nm (BA).

2.2.10. Calculation of skin permeation parameters

The flux of skin permeation experiment was calculated from drug permeation profile through the skin. Then, permeability coefficient of drug was obtained from division of flux by applied drug concentration, Cv (equation 4).

$$P = \frac{Flux}{C_v} \qquad\qquad\qquad \text{….. (4)}$$

Drug concentration in HF was supposed to be values calculated by eq. 5 as follows:

Drug concentration in HF (µmol/g)

$$= \frac{\text{Total amount of drug extracted from 30 hairs (µmol)}}{\text{Total weight of 30 hairs removed from the effetive peremation area}} \quad \dots\dots \quad (5)$$

2.2.11. Confocal Laser Scanning Microscope Observation

After topical application of Cal-Na and rhodamin over 8 h, the donor solution was immediately removed from the skin surface and the skin section was prepared with a cryotome (CM3050S; Leica Microsystems Inc., Tokyo, Japan). The cryostat skin section with the stratum corneum side up was examined using a confocal laser scanning microscope (CLSM, Fluoview FV1000; Olympus Corp., Tokyo, Japan). Cal was excited using an argon laser at an excitation wavelength of 488 nm, whereas rhodamine was excited by 543 nm helium–neon laser.

2.3. Results

2.3.1. In vitro skin permeation of drugs

Table 2.2 shows relationships P values of topically applied drugs through intact and stripped pig ear skin, respectively. P values of lipophilic chemicals ($\log K_{o/w} \geq 0$), BP (pH7.4), BA (pH3.0) and LC (pH10.0), through intact skin were 21.8×10^{-7}, 35.7×10^{-7} and 13.6×10^{-7} cm/s, respectively. On the other hand, P values of those compounds through stripped skin were 16.1×10^{-7}, 93.1×10^{-7} and 64.2×10^{-7} cm/s, respectively. P values through stripped skin were not so higher than those through intact skin. Especially, P value of BP permeations through intact skin were a little higher than that through stripped skin.

Table 2.2. Permeability coefficient of drugs through pig ear full-thickness skin and stripped skin. Values are the mean ± S.D. (n = 3-5).

Drug	$\log K_{o/w}$	Applied dose/1.77 cm^2	P values in full-thickness skin ($\times 10^{-7}$ cm/s)	P values in stripped skin ($\times 10^{-6}$ cm/s)
Cal-Na (pH 7.4)	-3.50	5 nmol	0.18 ± 0.04	2.51 ± 0.49
CP (pH 10.0)	-2.27	100 nmol	0.30 ± 0.14	3.61 ± 0.27
LC (pH 5.0)	-0.90	100 nmol	0.34 ± 0.09	4.67 ± 1.17
BA (pH 7.4)	-0.41	30 nmol	1.53 ± 0.35	11.8 ± 2.38
ISMN (pH 7.4)	-0.20	50 nmol	1.19 ± 0.35	5.10 ± 0.35
LC (pH 10.0)	1.40	100 nmol	13.6 ± 4.66	6.42 ± 1.63
BA (pH 3.0)	1.90	10 nmol	35.7 ± 4.67	9.31 ± 1.07
BP (pH 7.4)	3.50	0.5 nmol	21.8 ± 8.94	1.61 ± 0.37

In case of skin permeation of hydrophilic compounds ($\log K_{o/w} < 0$), on the other hand, P values of hydrophilic compounds, ISMN (pH 7.4), BA (pH 7.4), LC (pH5.0), CP (pH10.0) and Cal-Na (pH7.4), were 1.19×10^{-7}, 1.53×10^{-7}, 0.34×10^{-7}, 0.30×10^{-7} and 0.18×10^{-7} cm/s, respectively. The P values of these hydrophilic chemicals through stripped skin was dramatically improved compared with full-thickness skin [ISMN (pH7.4); 51.0×10^{-7}, BA (pH 7.4); 118×10^{-7}, LC (pH5.0); 46.7×10^{-7}, CP (pH10.0); 36.7×10^{-7} and Ca-Na (pH7.4); 25.1×10^{-7} cm/s, respectively].

2.3.2. *Changes in flux of skin permeation and hair follicle concentration of lipophilic drugs*

Figure 2.1 shows changes in flux of skin permeation of lipophilic drugs through intact skin (closed circle) and drug concentrations in HF (open square). Flux of lipophilic drugs (ISDN and BA) became that steady-state 4 h after topical application (Fig 1a, b). The supposed concentration profiles of drugs in HF were increased with an increase of time, and then each drug concentration showed the constant value as steady-state fluxes were observed for skin permeation (Fig 1a, b). On the other hand, BP concentration of in HF markedly increased immediately after topical application (1c), but the steady-state *flux* of BP was not obtained in 10 h after application.

2.3.3 *Changes in flux of skin permeation and hair follicle concentration of hydrophilic drugs*

Figure 2.2 shows changes in flux of skin permeation of hydrophilic drugs

through intact skin and drug concentrations in HF. Steady-state of fluxes were observed

for ISMN, BA and LC, whereas they were not observed for CP and Cal-Na. On the other

hand, drug concentrations in HF were rapidly increased after topical application, and then

steady-state concentrations in HF were achieved.

Fig. 2.1.   Time courses of HF concentration and *flux* through pig ear skin of a) ISDN (pH

7.4), b) BA (pH 3.0) and c) BP (pH 7.4) after topical application. Symbols: *flux* (●), drug

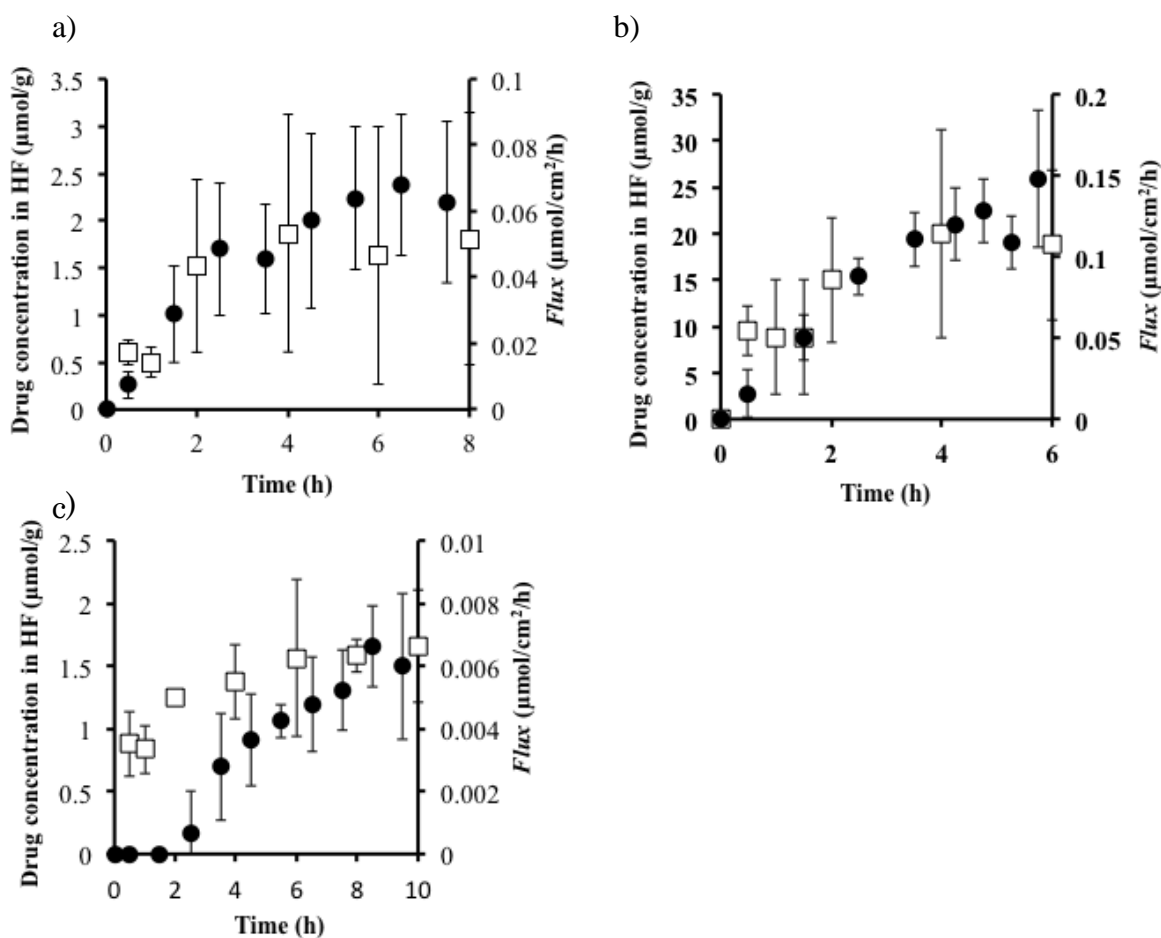concentration in HF (□). Each point shows the means ± S.D. (n = 3-6).
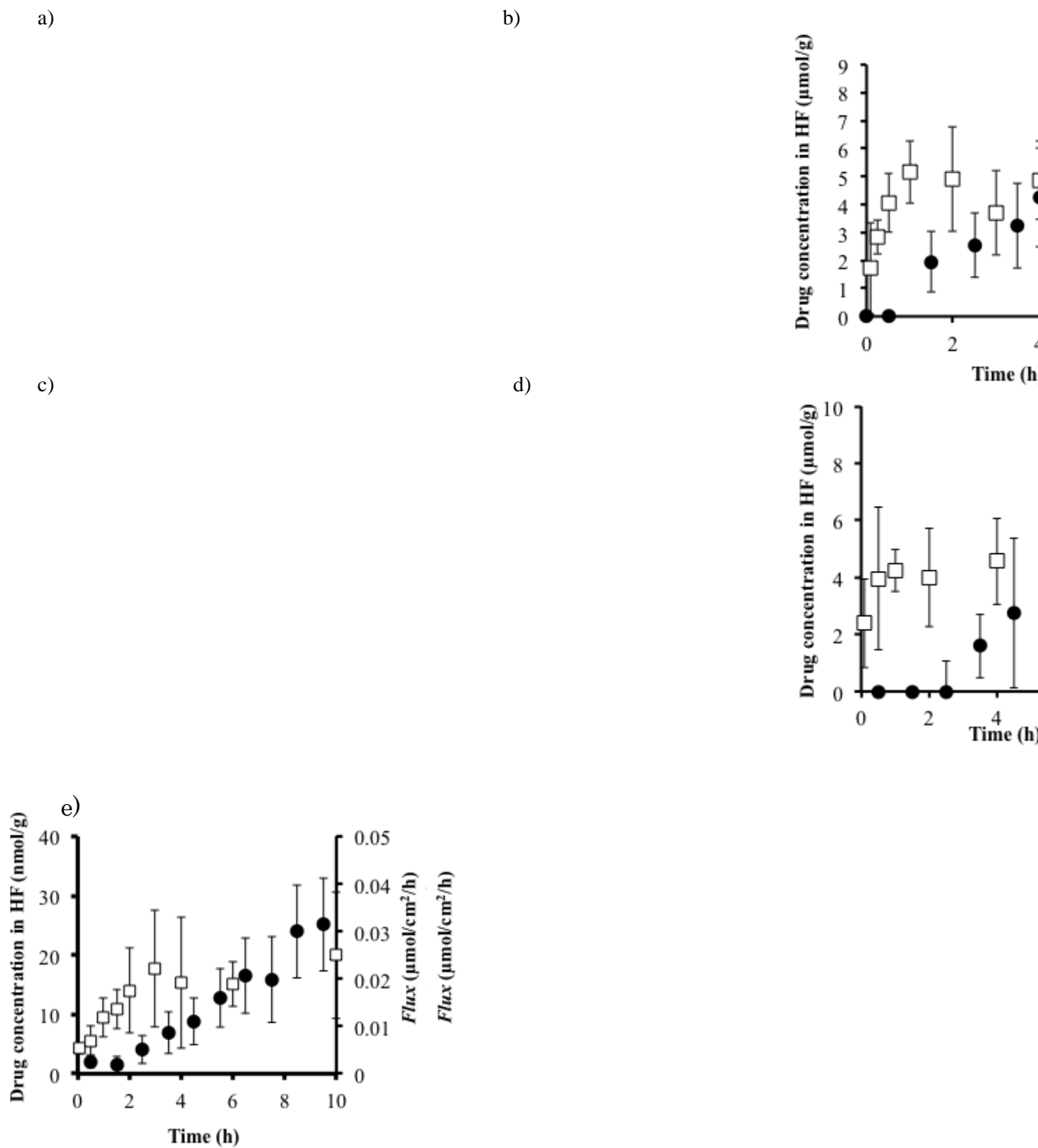
a)

b)

c)

d)

e)

Fig. 2.2. Time courses of HF concentration and *flux* through pig ear skin of a) ISMN (pH 7.4), b) BA (pH 7.4), c) LC (pH 5.0), d) CP (pH 10.0) and e) Cal-Na (pH 7.4) after topical application. Symbols: the same in Fig. 2.1. Each point shows the means ± S.D. (n = 3-6).

2.3.4. Skin disposition of drugs

Rhodamin or Cal-Na, a lipophilic or hydrophilic fluorescent maker, respectively, was topically applied to skin and the drug distribution was observed with a confocal laser scanning microscopy immediately after preparation of skin section. Rhodamin was observed both into the stratum corneum and HF, whereas Cal was slightly distributed in the stratum corneum and was much observed in the shallower part of HF and the HF shaft, as shown in Fig. 2.3.
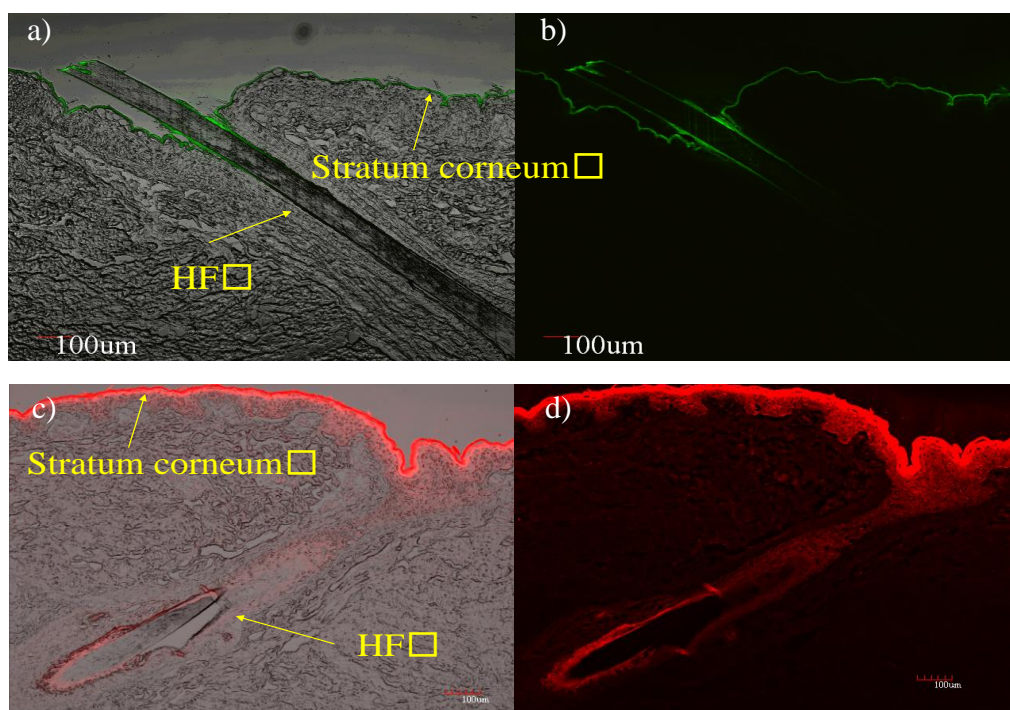

Fig. 2. 3. Conformal microscopic observation of Cal (a and b) and rhodamin (c and d) in the skin. a and c were merged with transmitted light and fluorescent images (b and d). Abbreviation of HF is HF.

2.3.5. Relationship between logKo/w and log (steady-state drug amount in hair follicles).

Figure 2.4 shows a relationship between log $K_{o/w}$ value of drugs and logarithm of steady-state drug amount in HF. The value of vertical axis was calculated from the division of steady-state drug amount in hair by the applied drug dose. In the present study, half of hairs, 30 hairs, were removed from the effective diffusion area （please see section 1. 60 hairs in average exist in the area）. Thus, two-fold the amount of extracted drugs from 30 hairs was used to calculate steady-state drug amount in HF. Drug amount in HF were increased with an increase of their lipophilicity, suggesting that the assumed HF was not simple aqueous phase. This relationship means that high amount would be delivered for lipophilic drugs compared with hydrophilic ones.
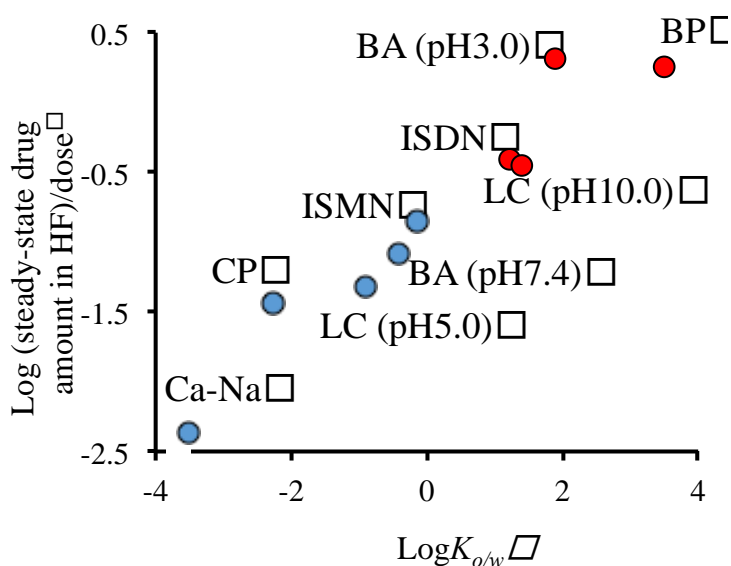

Fig. 2.4.   Relationship between log$K_{o/w}$ and log (steady-state drug amount in HF).

2.4. Discussion and chapter conclusion

Dermatopharmacokinetics is used to evaluate bioequivalence of topically applied drugs by a tape-stripping method[49, 64]. Furthermore, a few reports have recently published that *in silico* approach to estimate skin concentration of drug with different physicochemical properties in viable epidermis and dermis[65, 66]. Considering skin as a homogeneous membrane, these researches supposed a direct relation between chemicals concentration and its effect. It is an evidence that Hill equation could be applied to reveal the relationship between cell viability of topically applied chemicals and its concentration in skin [67].

Scheuplein reported that distribution of drugs into the HF would be occurred at the beginning process of skin permeation, although HF accounted only approximately 0.1 % of are against the total skin surface[68]. In addition, cyanoacrylate biopsy method was used to evaluate effect and safety of topically applied or exposed chemicals by investigating their concentrations in HF. However, in spite of the present measurements of drug concentration in stratum corneum and viable epidermis/dermis, few studies have been published on the drug concentration in the HF.

In this chapter, drug amount extracted from a removal hair was supposed to be that in the HF. Although this assumption is not fully right, we do not have any better or best determination method or tool for assessment of HF concentration of topically applied or exposed chemicals. Development of the technique or tool for assessing the follicle concentration of chemicals must be a future issue in this or related topics.

Delayed lag time of HF concentration for lipophilic drugs was observed

compared with those for hydrophilic ones. The time to become steady-state concentration of hydrophilic drugs in HF was much faster than those for fluxes. HF would be assumed to water-filled pore route [19]. Therefore, comparatively rapid distribution of hydrophilic drugs into HF might be occurred compared with lipophilic ones. On other hand, lipophilic drugs except for BP showed almost the same profiles between concentration in HF and skin permeation flux. It might be related to high distribution of lipophilic drugs into the HF from viable epidermis and dermis.

In the present experiment, drug distribution in HF was not observed after topical application of rhodamin and Cal-Na to HF-plugged skin. Thus, distribution profile of hydrophilic and lipophilic drugs could not be confirmed. Concentration profile of lipophilic drugs in HF should be the same to hydrophilic ones, because partitioning is a physical phenomenon. To reveal a relationship between physicochemical properties and HF concentration of drug in more detail, further experiments should be conducted. However, this chapter would markedly provide a new strategy for development of drug formulations having HF targeting ability.

General conclusions

The contribution of HF pathway on the skin permeation of chemicals was calculated from a difference between their permeability coefficients through skin with and without HF plugging using *in vitro* skin permeation experiment. The obtained results revealed that the contribution of HF pathway could be predicted by their lipophilicities. In a hydrophilic region of chemicals ($\log K_{o/w} < 0$), a higher reduction ratio was observed by HF plugging compared with lipophilic chemicals ($\log K_{o/w} \geq 0$). In addition, the reduction ratio was decreased with an increase in the $\log K_{o/w}$. This consideration on the HF pathway would be helpful to investigate usefulness and safety of chemicals after their topical application and exposure, because skin permeation and disposition must be changed at different sites of skin due to different sites and densities of HF.

Furthermore, another study was conducted to evaluate the drug disposition in HF. HF concentration of drugs with different lipophilicities was investigated to evaluate the effect of physicochemical properties on their HF disposition, where drugs having $\log K_{o/w} < 0$ and $\log K_{o/w} \geq 0$ were assumed to be lipophilic and hydrophilic, respectively. Results showed that the lag time observed in the skin permeation before obtaining a steady-state profile for hydrophilic drugs was delayed compared with that for lipophilic drugs. Hydrophilic drugs were found to be distributed through the HF as well as into the shallow part of stratum corneum, whereas lipophilic drugs distributed both into the stratum corneum and HF from a histological observation using fluorescent makers. These results suggest that lipophilic drugs could be easily delivered both into the stratum corneum and HF, whereas hydrophilic drugs were mainly delivered through HF, but not for deep layer of the stratum corneum.

Generally, stratum corneum route is the main permeation pathway for lipophilic drugs and HF route is the main permeation pathway for hydrophilic drugs. However lipophilic drugs will a give higher amount of drugs deposited at HF. The amount of hydrophilic drugs was not so high in HF. Therefore suitable drug delivery systems to treat acne need to be considered in detail from now on. Acne vulgaris is a very common skin disease, which causes a high degree of psychosocial suffering and has a detrimental effect on the quality of life for the patients irrespective of their age or gender.

Treatment of acne is principally directed towards these known pathogenic factors. Clindamycin and erythromycin are of commonly prescribed topical antibiotics for acne vulgaris with anti-inflammatory properties, among which the efficacy of clindamycin has remained better over a period of time. However, the effectiveness of acne treatments has been limited by their relative inability to penetrate into the pilosebaceous unit, the site of acne formation. By understanding characteristics of drugs and vehicles through this research, an efficient delivery to HF would be feasible in the near feature. In Appendix, I would like to show a possible formulation design for acne treatment.

Appendix

Using nano-emulsion formulation approach to enhance the skin permeation of

clindamycin and tetracycline as a new strategy for acne therapy.

A.1. Introduction

Selective HF delivery of topically applied drugs has been investigated with size-controlled particles. Many reports have been published that size-controlled particles (less than 10 μm) accumulated in the HF and the number of particles delivered to deeper area of HF was increased with a decrease of their particle size. The same principal has been used for adapalene gel, one of the acne care drug in the market, by containing size-controlled tretinoin particles (3 to 10 μm) in the formulation. Formulation design has been performed for selective HF delivery for topical application drugs with nanoparticles and lipid nano-vehicles.

Contribution of hair follicular pathway of topically applied medication can be useful to formulate the topically applied medication and to treat the acne. Development of nano-emulsion formulation to enhance skin permeation and HF concentration after topical application was investigated by Allec *et al.*[69]. In their study, the desirable particles (3 to 10 μm in diameter) were fabricated for HF delivery as shown in Fig. A..1.
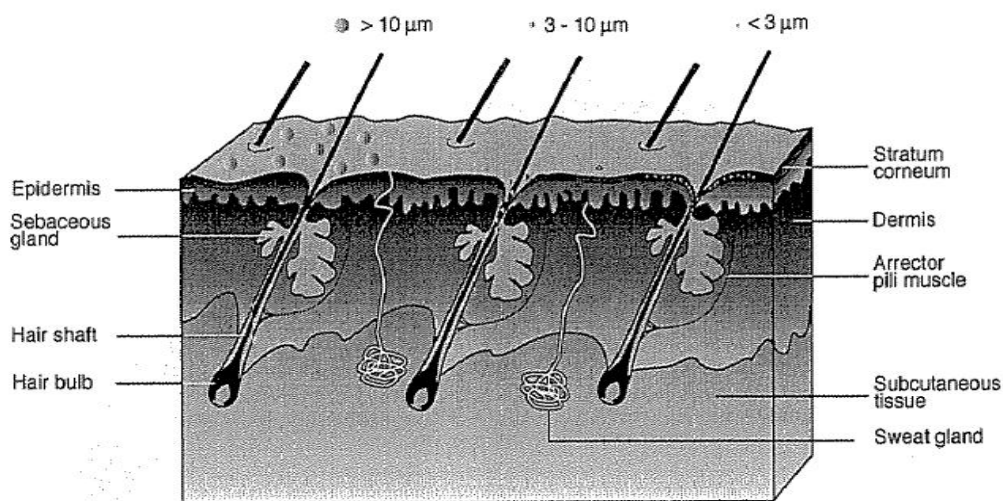
Fig. A..1. Desirable particle size (3 to 10 μm in diameter) for HF delivery usig Differin (adapalene) Gel containing tretinoin.

Anti-acne hydrophilic drugs, clindamycin phosphate, tetracycline HCl and gentamicin sulfate are not preferable for acne therapy due to difficult to deposition into HF, as shown in the 2nd chapter. Efficient acne therapy could be obtained by development of novel lipophilic drugs for acne therapy or by design of formulations with lipophilic vehicles such as nano-emulsions.

Nano-emulsions consist of fine oil-in-water or water-in-oil dispersions, having droplets covering the size range of 10-600 nm. Nano-emulsion can be used for pharmaceuticals and biomedical aids. These vehicles especially show great promise for the future of cosmetics, diagnostics, drug therapies and biotechnologies.

The aim of this work was to formulate the clindamycin and tetracycline nano-emulsions by emulsion phase inversion method and olive oil as an oil phase to increase the effectiveness of acne treatment through the increase the penetration of the active

compounds inside the lipophilic environment of the pilosebaceous unit.

A..2 Method

A..2.1. Materials

Clindamycin phosphate and tetracycline were provided by Y.S.P. Industries (M) Sdn. Bhd., CIRIO® olive oil from local supermarket, and polyethylene glycol sorbitan monooleate (Tween®80), sorbitan monolaurate (Span®20), methyl paraben and distilled water were obtained from the Management and Science University, Pharmacy Laboratory.

A..2.2. Apparatus

Laser diffractometer Mastersizer 2000 with the Hydro 2000SM module (Malvern Instruments, UK) and Brookfield RS portable rheometer with Coxial CC3-14 Spindle were used in this experiment.

A..2.3. Pre-formulation studies pseudo-ternary phase diagram

All emulsions were prepared by according the emulsion phase inversion method, where the water and oil phases were separately heated at 75°C, the water phase was added into the oil phase (olive oil, clindamycin phosphate and mixture of surfactants) while stirred at 600 rpm, and the mixture was then cooled to 25°C while stirring. Figure A..2 shows flow diagram of this preparation method.

Surfactant (Tween®) and co-surfactant (Span®20) were mixed at fixed mass ratio (1:1) which was then labeled as mixture of surfactant (Smix). For the phase diagram, oil,

distilled water and Smix at a specific ratio was mixed thoroughly at different mass ratios. Twenty one different combinations of oil, distilled water and Smix were made, so that the maximum ratios can be covered for this study.

The physical state of the nano-emulsion was marked on a pseudo-three-component phase diagram with one axis representing the aqueous phase, the second one representing oil and the third representing a mixture of surfactant and co-surfactant at a fixed mass ratio. Figures A..3 and A..4 are the pseudo-ternary phase diagram for clindamycin and tetracycline to develop nano-emulsion formulations.
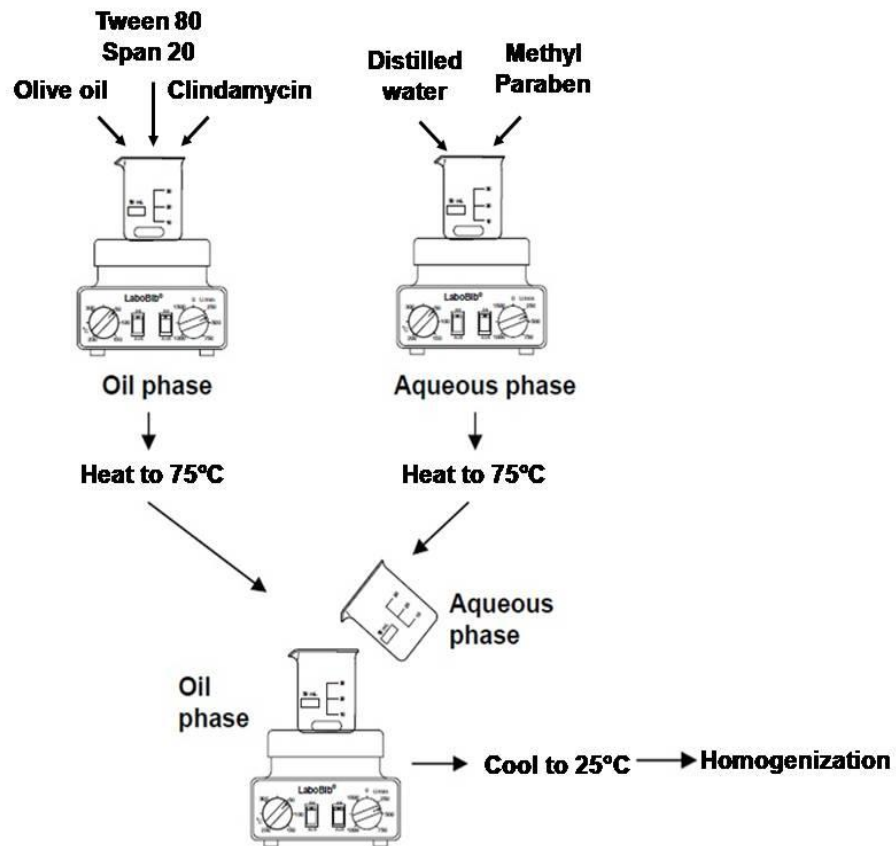
Fig. A..2. Preparation flow of nano-emulsion using emulsion phase inversion method.
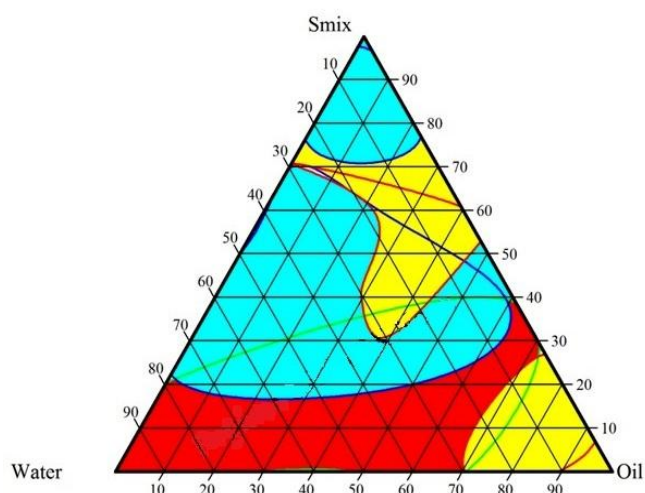
Fig. A..3.   Pseudo ternary phase diagram of clindamycin emulsion with olive oil, water and mixture of surfactant (Tween® 80 and Span® 20). Red region shows non-transparent emulsion, yellow region is transparent gel, and blue region shows viscous region.
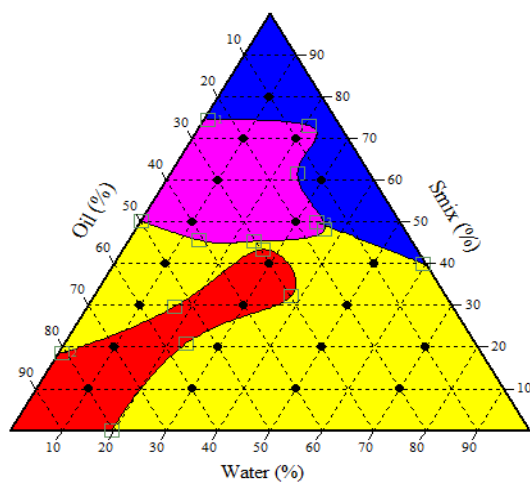

Fig. A..4. Pseudo ternary phase diagram of tetracycline emulsion. Four different areas were observed. The pink area represents a clear one homogenous preparation, the blue area represents cloudy creamy preparation, the yellow represents cream preparation and the red area shows the phase separation area.

A..3. Result

A..3.1 Formulation.

Three best formulations were selected to be candidates to proceed further experiments. Table A..1 shows the best 3 formulations with suitable of physical characteristics as nano-emulsions.

Table A..1. Selected formula of nano-emulsions to be used to determine particle size.

Ingredients	F8 (%)	F17 (%)	F18 (%)
Clindamycin phosphate or tetracycline	1	1	1
Methyl paraben	1	1	1
Olive oil	8	28	8
Mixture of surfactant (1:1)	20	60	60
Distilled water	70	10	30

These 3 formulations of clindamycin and tetracycline emulsions were selected to be the best formulations which produce the nano-sized droplets which can easily penetrate into HF after application on the skin surface.

A..3.2. Mean droplet size of clindamycin and tetracycline nano-emulsions

In the three selected nano-emulsions shown in Table A..2, the particle size was analyzed by a laser diffractometer Mastersizer 2000 with the Hydro 2000SM module (Malvern Instruments, UK).

Table A..2. Particle size of the selected emulsions

Formula	Mean droplet size of clindamycin emulsion	Mean droplet size of tetracycline emulsion
Formula 8	0.9 micron	0.5 micron
Formula 17	41.6 micron	5 micron
Formula 18	44.6 micron	60 micron

From the results, all the three formulations (F8, F17 and F18) showed the mean droplet size below 45 μm. The mean droplet size of the micro-emulsions was between 0.920 μm to 44.695 μm. The average size of F8, F17 and F18 were 0.920 μm, 41.647 μm and 44.695 μm, respectively.

The droplet size increased with increases in oil concentration and Smix concentration in the formulations. The droplet size of formulation F8, containing 10% of oil and 20% on Smix was 0.920 μm, which was lower as compared to other formulations. Only a marginal difference was observed in the mean droplet size of formulations F17 and F18, which may be due to the equal concentration of Smix (60%) in both the formulations.

A.4. Discussion

Clindamycin and tetracycline nano-emulsions were not obtained using the emulsion phase inversion method in this study. The emulsions that produced in this study were all in the micro-range. This result is in accordance with a report that the addition of surfactant to micro-emulsion systems caused the interfacial film to condense and stabilize, while the co-surfactant caused the film to expand [22]. All the formulations in the present study had droplets in the micro range.

A.5. Appendix conclusion

Clindamycin emulsion and tetracycline emulsion with suitable particle sizes were obtained using the emulsion phase inversion method for HF route delivery. Further studies to evaluate efficiency of nano-emulsion formulation as a vehicle to deliver hydrophilic drugs to HF, especially as drugs foracne treatment, or looking for the best formulation to deliver both hydrophilic and lipophilic drugs to treat acne will be needed.

Acknowledgments

References

1. Alvarez-Roman R., Naik A., Kalia Y. N., Guy R. H., Fessi H., Skin penetration and distribution of polymeric nanoparticles, *J. Control. Release*, **99**, 53–62 (2004).

2. Gawkrodger, D. J., Dermatology: an illustrated color text, 3rd ed. (2002).

3. Anderson B. D., Raykar P. V., Solute structure-permeability relationships in human stratum corneum, *J. Invest. Dermatol.*, **93**, 280–286 (1989).

4. Błędzka D., Gryglik D., Miller J. S., Photodegradation of butylparaben in aqueous solutions by 254 nm irradiation, *J. Photochem. Photobiol.*, **A 203**, 131–136 (2009).

5. Buchwald P., Bodor N., A simple, predictive, structure-based skin permeability model, *J. Pharm. Pharmacol.*, **53**, 1087–1098 (2001).

6. Cazares-Delgadillo J., Naik A., Kalia Y. N., Quintanar-Guerrero D., Ganem-Quintanar A., Skin permeation enhancement by sucrose esters: a pH dependent phenomenon, *Int. J. Pharm.*, **297**, 204–212 (2005).

7. Jacobi U., Tassopoulos T., Surber C., Lademann J., Cutaneous distribution and localization of dyes affected by vehicles all with different lipophilicity, *Arch Dermatol Res.*, **297**, 303–310 (2006).

8. Cole L., Coleman J., Evans D., Hawes C., Internalisation of fluorescein isothiocyanate and fluorescein isothiocyanatedextran by suspension-cultured plant cells, *Journal of Cell Sci.*, **96**, 721–730 (1990).

9. Crank J., The Mathematics of Diffusion, Oxford University Press (1979).

10. Domanska U., Pobudkowska A., *pK*a and solubility of drugs in water, ethanol, and 1-octanol, *J. Phys. Chem. B.*, **113**, 8941–8947 (2009).

11. Essa E. A., Bonner M. C., Barry B. W., Human skin sandwich for assessing shunt route penetration during passive and iontophoretic drug and liposome delivery, *J. Pharm. Pharmacol.*, **54**, 1481–1490 (2002).

12. Frldman R. J., Maibach H. I., Regional variation in percutaneous penetration of 14 C cortisol in man, Regional variation in percutaneous penetration of 14 C cortisol in man, *J. Invest. Dermatol.*, **48**, 181–183 (1967).

13. Naik A., Kalia Y., Guy R., Transdermal drug delivery: overcoming the skin's barrier function, *Pharm. Sci. Technol. Today.,* **3**, 318–326 (2000).

14. Pappas A., Epidermal surface lipids, *Dermatoendocrinol*, **1**, 72–76 (2009).

15. Mizutani Y., Mitsutake S., Tsuji K., Kihara A., Igarashi Y., Ceramide biosynthesis in keratinocyte and its role in skin function, *Biochimie*, **91**, 784–790 (2009).

16. Scheuplein R.J., Mechanism of percutaneous absorption. II. Transient diffusion and the relative importance of various routes of skin penetration, *J. Invest. Dermatol.*, **48**, 79–88. (1967).

17. Mitragotri S., Modeling skin permeability to hydrophilic and hydrophobic solutes based on four permeation pathways, *J. Control. Release*, **86**, 69–92 (2003).

18. Wosicka H., Cal K., Targeting to the hair follicles: Current status and potential, *J. Dermatol. Sci.,* **57**, 83–89 (2010).

19. Todo H., Kimura E., Yasuno H., Tokudome Y., Hashimoto F., Ikarashi Y., Sugibayashi K., Permeation pathway of macromolecules and nanospheres through skin, *Biol. Pharm. Bull.*, **33**, 1394–1399 (2010).

20. Maibach H. I., Feldman R. J., Milby T. H., Serat W. F., Regional variation in

percutaneous penetration in man. Pesticides, *Arch. Environ. Health*, **23**, 208–211 (1971).

21. Hueber F., Wepierre J., Schaefer H., Role of transepidermal and transfollicular routes in percutaneous absorption of hydrocortisone and testosterone: *in vivo* study in the hairless rat, *Skin Pharmacol.*, **5**, 99–107 (1992).

22. J. E. Grice, S. Ciotti, N. Weiner, P. lockwood, S. E. Cross, M. S. Roberts, Relative uptake of minoxidil into appendages and stratum corneum and permeation through human skin *in vitro*, *J. Pharm. Sci.*, **99**, 712-8 (2010).

23. Ogiso T., Shiraki T., Okajima K., Tanino T., Iwaki M., Wada T., Transfollicular drug delivery: penetration of drugs through human scalp skin and comparison of penetration between scalp and abdominal skins *in vitro*, *J. Drug Target.*, **10**, 369–378 (2002).

24. Lieb L. M., Liimatta A. P., Bryan R. N., Brown B. D., Krueger G. G., Description of the intrafollicular delivery of large molecular weight molecules to follicles of human scalp skin *in vitro*, *J. Pharm. Sci.*, **86**, 1022–1029 (1997).

25. Liu X., Grice J. E., Lademann J., Otberg N., Trauer S., Patzelt A., Roberts M. S., Hair follicles contribute significantly to penetration through human skin only at times soon after application as a solvent deposited solid in man, *B. J. Clin. Pharmacol.*, **72**, 768–774 (2011).

26. Frum Y., Bonner M. C., Eccleston G. M., Meidan V. M., The influence of drug partition coefficient on follicular penetration: in vitro human skin studies, *Eur. J. Pharm. Sci.*, **30**, 280–287 (2007).

27. Horita D., Yoshimoto M., Todo H., Sugibayashi K., Analysis of hair follicle

penetration of lidocaine and fluorescein isothiocyanate-dextran 4 kDa using hair follicle-plugging method, *Drug Dev. Ind. Pharm.,* **40**, 345–351 (2014).

28. Otberg N., Patzelt A., Rasulev U., Hagemeister T., Linscheid M., Sinkgraven R., Sterry W., Lademann J., The role of hair follicles in the percutaneous absorption of caffeine, *B. J. C. Pharmacol.*, **65**, 488–492 (2008).

29. Trauer S., Patzelt A., Otberg N., Knorr F., Rozycki C., Balizs G., Buttemeyer R., Linscheid M., Liebsch M., Lademann J., Permeation of topically applied caffeine through human skin; a comparison of *in vivo* and *in vitro* data, *Br. J. Clin. Pharmacol.,* **68**, 181–186 (2009).

30. Takeuchi H., Takeuchi H., Ishida M., Ishida M., Furuya A., Furuya A., Todo H., Urano H., Sugibayashi K., Influence of skin thickness on the *in vitro* permeabilities of drugs through Sprague-Dawley rat or Yucatan micropig skin, *Biol. Pharm. Bull.*, **35**, 192–202 (2011).

31. Yamada K., Yamashita J., Todo H., Miyamoto K., Hashimoto S., Tokudome Y., Hashimoto F., Sugibayashi K., Preparation and evaluation of liquid-crystal formulations with skin-permeation-enhancing abilities for entrapped drugs, *J. Oleo. Sci.,* **60**, 31–40 (2010).

32. Sugibayashi K., Todo H., Oshizaka T., Owada Y., Mathematical model to predict skin concentration of drugs: toward utilization of silicone membrane to predict skin concentration of drugs as an animal testing alternative, *Pharm. Res.,* **27**, 134-142 (2010).

33. Heger M., Salles I. I., van Vuure W., Deckmyn H., Beek J. F., Fluorescent labeling of

platelets with polyanionic fluorescein derivatives, *Anal. Quant. Cytol. Histol.*, **31**, 227–232 (2009).

34. Kolthoff I. M., Stenger V. A., Volumetric Analysis, vol. 1, Interscience Publishers, New York (1942).

35. Tamura M., Sueishi T., Sugibayashi K., Morimoto Y., Juni K., Hasegawa T., Kawaguchi T., Metabolism of testosterone and its ester derivatives in organotypic coculture of human dermal fibroblasts with differentiated epidermis, *Int. J. Pharm.*, **131**, 263–271. (1995).

36. Ahmed S., Imai T., Otagiri M., Evaluation of stereo selective transdermal transport and concurrent cutaneous hydrolysis of several ester prodrugs of propranolol: Mechanism of stereoselective permeation. *Pharm. Res.*, **13**, 1524–1529 (1996).

37. Sugibayashi K., Hayashi T., Matsumoto K., Hasegawa T., Utility of a three dimensional cultured human skin model as a tool to evaluate the simultaneous diffusion and metabolism of ethyl nicotinate in skin, *Drug Metab. Pharmacokinet.*, **19**, 352–362 (2004).

38. Hashida M., Okamoto H., Sezaki H., Analysis of drug penetration through skin considering donor concentration decrease, *J. Pharmacobio.-Dyn.*, **11**, 636–644 (1988).

39. Okamoto, H., Hashida, M., Sezaki, H., Structure-activity relationship of 1-alkyl- or 1-alkenylazacycloalkanone derivatives as percutaneous penetration enhancers, *J. Pharm. Sci.*, **77**, 418–424. (1988).

40. Sato K., Oda T., Sugibayashi K., Morimoto Y., Estimation of blood concentration of drugs after topical application from in vitro skin permeation data. I. Prediction by

convolution and confirmation by deconvolution, *Chem. Pharm. Bull*., **36**, 2232–2238. (1988).

41. Guy R. H., Hadgraft J., Pharmacokinetic interpretation of the plasma levels of clonidine following transdermal delivery, *J. Pharm. Sci*., **74**, 1016–1018 (1985).

42. Yamashita F., Bando H., Koyama Y., Kitagawa S., Takakura Y., Hashida M., *In vivo* and *in vitro* analysis of skin penetration enhancement based on a two-layer diffusion model with polar and nonpolar routes in the stratum corneum, *Pharm. Res.,* **11**, 185–191 (1994).

43. Patzelt A., Richter H., Buettemeyer R., Huber H. J. R., Blume-Peytavi U., Sterry W., Lademann J., Differential stripping demonstrates a significant reduction of the hair follicle reservoir in vitro compared to *in vivo*, *Eur. J. Pharm. Biopharm*., **70**, 234–238 (2008).

44. Raber A.S., Mittal A., Schafer, J., Bakowsky U., Reichrath J., Vogt T., Schaefer U. F., Hansen S., Lehr C. M., Quantification of nanoparticle uptake into hair follicles in pig ear and human forearm, *J. Control. Release*, **179**, 25–32. (2014).

45. Warner R. R., Stone K. J., Boissy Y. L., Hydration disrupts human stratum corneum ultrastructure, *J. Invest. Dermatol.,* **120**, 275–284 (2003).

46. Kiistala U., Suction blister device for separation of viable epidermis from dermis, *J. Invest. Dermatol.*, **50**, 129-137 (1968).

47. Surber C., Wilhelm K. P., Bermann D., Maibach H. I., *In vivo* skin penetration of acitretin in volunteers using three sampling techniques, *Pharm. Res.*, **10**, 1291-1294 (1993).

48. Laugier J. P., Surber C., Bun H., Geiger J. M., Wilhelm K. P., Durand A., Maibach H.I., Determination of acitretin in the skin, in the suction blister, and in plasma of human volunteers after multiple oral dosing, *J. Pharm. Sci.*, **83**, 623-628 (1994).

49. N'Dri-Stempfer B., Navidi W. C., Guy R. H., Bunge A. L., Improved bioequivalence assessment of topical dermatological drug products using dermatopharmacokinetics, *Pharm. Res.*, **26**, 316-328 (2009).

50. Kalia Y. N., Pirot F., Guy R. H., Homogeneous transport in a heterogeneous membrane: water diffusion across human stratum corneum, *in vivo*, *Biophys. J.*, **71**, 2692-2700 (1996).

51. Rougier A., Dupuis D., Lotte C., Roguet R., Schaefer H., *In vivo* correlation between stratum corneum reservoir function and percutaneous absorption, *J. Invest. Dermatol.*, **81**, 275-278 (1983).

52. Surber C., Wilhelm K. P., Hori M., Maibach H. I., Guy R. H., Optimization of topical therapy: partitioning of drugs into stratum corneum, *Pharm. Res.*, **7**, 1320-1324 (1990).

53. Kassis V., Sondergaard J., Heat-separation of normal human skin for epidermal and dermal prostaglandin analysis, *Arch. Dermatol. Res.*, **273**, 301-306 (1982).

54. Bidmon H. J., Pitts J. D., Solomon H. F., Bondi J. V., Stumpf W. E., Estradiol distribution and penetration in rat skin after topical application, studied by high resolution autoradiography, *Histochem.*, **95**, 43-54 (1990).

55. Yamada K., Yamashita J., Todo H., Miyamoto K., Hashimoto S., Tokudome Y., Hashimoto F., Sugibayashi K., Preparation and evaluation of liquid-crystal formulations with skin permeation-enhancing abilities for entrapped drugs, *J. Oleo Sci.*,

60, 31-40 (2010).

56. Mori K., Hasegawa T., Sato S., Sugibayashi K., Effect of electric field on the enhanced skin permeation of drugs by electroporation, *J. Control Release*, **90**, 171-179 (2003).

57. Dorota B., Dorota G., Jacek S. M., Photodegradation of butylparaben in aqueous solutions by 254 nm irradiation, *J. Photochem. Photobiol A: Chemistry*, **203**, 131-136 (2009).

58. Cazares-Delgadillo J., Naik A., Kalia Y. N., Quintanar-Guerrero D., Ganem-Quintanar A., Skin permeation enhancement by sucrose esters: a pH-dependent phenomenon, *Int. J. Pharm.*, **297**, 204-212 (2005).

59. Connors K. A., Connors K. A., Amidon G. L., Stella V. J., Chemical Stability of Pharmaceuticals: A Handbook for Pharmacists, John Wiley & Sons, 1986.

60. Heger M., Salles I. I., Van V. W., Deckmyn H., Beek J. F., Fluorescent labeling of platelets with polyanionic fluorescein derivatives, *Anal. Quant. Cytol. Histol.*, **31**, 227-232 (2009).

61. Tamura M., Sueishi T., Sugibayashi K., Morimoto Y., Juni K., Hasegawa T., Kawaguchi T., Metabolism of testosterone and its ester derivatives in organotypic coculture of human dermal fibroblasts with differentiated epidermis, *Int. J. Pharm.*, **131**, 263–271 (1996).

62. Ahmed S., Imai T., Otagiri M., Evaluation of stereoselective transdermal transport and concurrent cutaneous hydrolysis of several ester prodrugs of propranolol: mechanism of stereoselective permeation, *Pharm Res.*, **13**, 1524-1529 (1996).

63. Sugibayashi K., Hayashi T., Matsumoto K., Hasegawa T., Utility of a three

dimensional cultured human skin model as a tool to evaluate the simultaneous diffusion and metabolism of ethyl nicotinate in skin, *Drug Metabol. Phamacokin.*, **19**, 352-362 (2004).

64. Herkenne C., Naik A., Kalia Y. N., Hadgraft J., Guy R. H., Pig ear skin *ex vivo* as a model for *in vivo* dermatopharmacokinetic studies in man, *Pharm. Res.*, **23**, 1850-1856 (2006).

65. Polak S., Ghobadi C., Mishra H., Ahamadi M., Patel N., Jamei M., Rostami-Hodjegan A., Prediction of concentration-time profile and its inter-individual variability following the dermal drug absorption, *J. Pharm. Sci.* **101**, 2584–2595 (2012).

66. Chen L., Han L., Saib O., Lian G., *In silico* prediction of percutaneous absorption and disposition kinetics of chemicals, *Pharm. Res.*, **32**, 1779–1793 (2015).

67. Kano S., Sugibayashi K., Kinetic analysis on the skin disposition of cytotoxicity as an index of skin irritation produced by cetylpyridinium chloride: comparison of *in vitro* data using a three-dimensional cultured human skin model with *in vivo* results in hairless mice, *Pharm. Res.*, **23**, 329–335 (2006).

68. Scheuplein R. J., Mechanism of percutaneous absorption. II. Transient diffusion and the relative importance of various routes of skin penetration, *J. Invest. Dermatol.,* **48**, 79–88 (1967).

69. Allec J., Chatelus A., Wagner N., Skin distribution and pharmaceutical aspects of adapalene gel, *J. Am. Acad. Dermatol.*, **36**,119-25, (1997).